Synthesis, Inhibitory Activity of Cholinesterases, and Neuroprotective Profile of Novel 1,8-Naphthyridine Derivatives

ARTICLE *in* JOURNAL OF MEDICINAL CHEMISTRY · JULY 2010

Impact Factor: 5.45 · DOI: 10.1021/jm901902w · Source: PubMed

Journal of Medicinal Chemistry Article

J. Med. Chem. **2010,** *53,* 5129–5143 **5129**
DOI: 10.1021/jm901902w

Synthesis, Inhibitory Activity of Cholinesterases, and Neuroprotective Profile of Novel 1,8-Naphthyridine Derivatives

Cristóbal de los Ríos,*[,†,‡,∥] Javier Egea,[†] José Marco-Contelles,*[,‡] Rafael León,[†,⊥] Abdelouahid Samadi,[‡] Isabel Iriepa,[∥] Ignacio Moraleda,[∥] Enrique Gálvez,[∥] Antonio G. García,[†,§] Manuela G. López,[†] Mercedes Villarroya,[†] and Alejandro Romero[†]

[†]*Departamento de Farmacología y Terapéutica, Facultad de Medicina, Instituto Teófilo Hernando, Universidad Autónoma de Madrid, C/Arzobispo Morcillo 4, 28029 Madrid, Spain,* [‡]*Laboratorio de Radicales Libres y Química Computacional, Instituto de Química Orgánica General, Consejo Superior de Investigaciones Científicas, C/Juan de la Cierva 3, 28006 Madrid, Spain,* [§]*Servicio de Farmacología Clínica, Hospital Universitario de la Princesa, C/Diego de León 62, 28006 Madrid, Spain, and* [∥]*Departamento de Química Orgánica, Facultad de Farmacia, Universidad de Alcalá de Henares, Ctra. Barcelona, Km. 33.5, 28817, Alcalá de Henares, Spain.* [⊥]*Current Address: Department of Chemistry, University of Cambridge Lensfield Road, Cambridge CB2 1EW, U.K.*

Received December 23, 2009

1,8-Naphthyridine derivatives related to **17** (ITH4012), a neuroprotective compound reported by our research group, have been synthesized. In general, they have shown better inhibition of acetylcholinesterase (AChE) and butyrylcholinesterase (BuChE) than most tacrine derivatives previously synthesized in our laboratory. The compounds presented an interesting neuroprotective profile in SH-SY5Y neuroblastoma cells stressed with rotenone/oligomycin A. Moreover, compound **14** (ethyl 5-amino-2-methyl-6,7,8,9-tetrahydrobenzo[*b*][1,8]naphthyridine-3-carboxylate) also caused protection in cells stressed with okadaic acid (OA) or amyloid β 1−42 peptide ($A\beta_{1-42}$). Interestingly, compound **14** prevented the OA-induced PP2A inhibition, one of the enzymes implicated in τ dephosphorylation. This compound also exhibited neuroprotection against neurotoxicity elicited by oxygen and glucose deprivation in hippocampal slices. Because these stressors caused neuronal damage related to physiopathological hallmarks found in the brain of Alzheimer's disease (AD) patients, we conclude that compound **14** deserves further in vivo studies in AD models to test its therapeutic potential in this disease.

Introduction

Alzheimer's disease (AD[a]) is an age-related neurodegenerative disease characterized by progressive memory loss, decline in language skills, and loss of function.[1] Although the etiology of AD is unknown, histopathological hallmarks such as amyloid β ($A\beta$) deposits,[2] τ-protein aggregation,[3] oxidative stress,[4] and low levels of acetylcholine (ACh) have been characterized.[5−7] Currently, there are four drugs for AD approved by regulatory agencies, three cholinesterase inhibitors (rivastigmine, donepezil and galantamine), and a NMDA receptor blocker (memantine).[8] Cholinesterase inhibitors can reduce AD symptoms by inhibiting acetylcholinesterase (AChE), the enzyme responsible for the hydrolysis of ACh at the synaptic cleft.[9] This therapeutic strategy is based on the so-called cholinergic hypothesis,[1] which suggests that the selective loss of cholinergic neurons in AD results in a deficit of ACh in specific areas of the brain that mediate learning and memory functions.[10]

There is no agreement in the scientific community about the benefits of the cholinergic therapy.[11,12] However, a renewed interest for AChE inhibitors arose when beneficial effects, not linked to cholinergic neurotransmission, were demonstrated for some of them.[13,14] For instance, galantamine has been described to protect human neuroblastoma cells[15] and cortical neurons against $A\beta$-induced neurotoxicity.[16] Furthermore, donepezil reduced τ-phosphorylation by inhibition of GSK-3β.[17] In addition, AChE seems to accelerate amyloid fibrils aggregation in the brain, forming stable complexes with $A\beta$;[18] this action involves the peripheral anionic binding site (PAS) of AChE.[19] These effects, together with the fact that AD pathogenesis appears to be multifactorial, have led to the current opinion that drugs with moderate activities acting on two or more targets will be more effective than a highly potent and selective drug acting on a single target.[20] The multitarget approach[21] includes tacrine−donepezil hybrids as $A\beta$ aggregation inhibitors,[22] coumarin or tacrine derivatives that inhibit both AChE and β-site APP cleaving enzyme (BACE1),[23,24] and highly potent neuroprotectant rasagiline−rivastigmine hybrids,[25] among many others.

During the past decade, we have devoted our effort to the design and synthesis of multitarget compounds and their biological evaluation as potential drugs for AD, based on the juxtaposition of the structures of tacrine and 1,4-dihydropyridines (1,4-DHPs). Up to now, we have described the synthesis and biological evaluation of 4*H*-pyranopyridines,[26] 1,8-naphthyridines,[27] and 1,4-dihydro[1,8]naphthyridines[28,29] (Chart 1).

*To whom correspondence should be addressed. For C.d.l.R.: phone, +34-91-4972766; fax, +34-91-4973120; e-mail, cristobal.delosrios@uam.es. For J.M.-C.: phone, +34-91-5622900; fax, +34-91-5644853; e-mail, iqoc21@iqog.csic.es.

[a] Abbreviations: 1,4-DHP, 1,4-dihydropyridine; $A\beta$, amyloid β peptide; ACh, acetylcholine; AChE, acetylcholinesterase; AD, Alzheimer's disease; APP, amyloid precursor protein; BACE-1, β-site of amyloid precursor protein cleaving enzyme; BDNF, brain-derived neurotrophic factor; BuChE, butyrylcholinesterase; GSK-3β, glucogen synthase kinase 3β; LDH, lactate dehydrogenase; NMDA, *N*-methyl-D-aspartate; OA, okadaic acid; OGD, oxygen and glucose deprivation; PAS, peripheral anionic binding site; rms, root mean square, VDCC, voltage-dependent calcium channel.

Published on Web 06/24/2010

Chart 1. Selected Tacrine−1,4-DHP Hybrids Described in Previous Papers

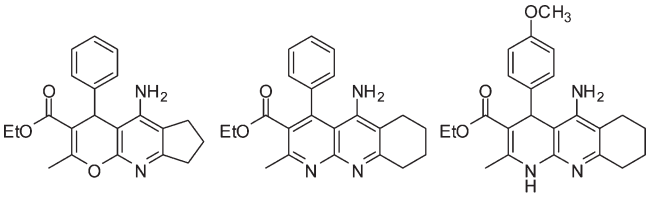

Chart 2. 1,8-Naphthyridines Based on the Juxtaposition of an AChE Inhibitor (Tacrine) and a 1,4-Dihydropyridine (Nifedipine)

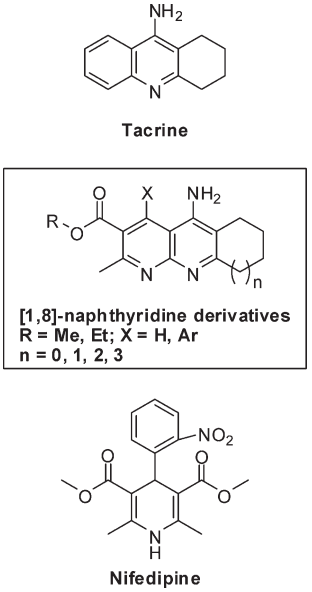

Tacrine (9-amino-1,2,3,4-tetrahydroacridine) was the first AChE inhibitor (AChEI) described,[30] while 1,4-DHPs are selective blockers of the L-type voltage-dependent Ca^{2+} channel (VDCC, $Ca_V1.1-1.4$).[31] 1,4-DHPs have exerted neuroprotection in several in vivo models of ischemia and neurodegeneration.[32,33] The hybrid compounds prepared in our laboratory have shown inhibitory activity of AChE and potent L-type VDCC blockade.[29,34] Additionally, they were able to protect neuroblastoma cells against various toxic stimuli, such as Aβ, veratridine, Ca^{2+} overload, H_2O_2, and thapsigargin.[29,35] One of them, the derivative **17** (ITH4012, Chart 1),[35] induced expression of the antiapoptotic protein Bcl-2 and the neurotrophic factor BDNF, activities that could be mediating its neuroprotective actions. Compound **17** was the most potent AChEI of its family but 4-fold less active than tacrine.[27] Docking studies suggested that the aromatic substituent at C4 of **17** might hinder passing through the gorge to reach the catalytic binding site of AChE.[34] These computational data prompted the design of a series of compounds lacking an aromatic substituent at C4 (X = H; Chart 2), thus favoring their accommodation into the AChE catalytic binding site and potentiating the inhibitory activity of cholinesterase enzymes. Therefore, we present in this paper the synthesis and pharmacological evaluation of novel 1,8-naphthyridine derivatives, analogues to compound **17** without substitution at C4. This implies an important modification from all of our previous studies. Thus, this series of compounds has been designed to find the first structural hits for further optimization, like cycloalkane-fused ring expansion or contraction (n = 0, 1, 2, 3; Chart 2) or the change in the carboxylic ester alkyl chain (R = Me, Et). Together with the synthesis and inhibitory activity on cholinesterase enzymes, we describe here the neuroprotective properties in two different models of cell death related to AD pathology, as well as their modulating activity of VDCCs.

Results and Discussion

Chemistry. For the synthesis of 1,8-naphthyridine precursors, we started from the conveniently substituted 2-pyridinones (Scheme 1), prepared as described by Abu-Shanab and co-workers.[36] Following the experimental procedure described for the synthesis of **2**, a mixture of **2** (17%) and the methyl ester derivative **1** as major compound (55%) was obtained. Compound **1** was presumably formed by transesterification process with methanol, generated in the reaction of ethyl acetoacetate with dimethylformamide dimethyl acetal. Compound **2** was chemoselectively prepared using dimethylformamide diethyl acetal instead, with medium yield (48%). As shown in the literature, we had scarcely studied structure−activity relationships by modifications at the alkyl ester.[26,27,29,34] Therefore, we considered using both methyl and ethyl esters to synthesize new 1,8-naphthyridine derivatives.

From the 2-pyridinone derivatives **1** and **2**, chlorination with phosphorus oxychloride[37] followed by aromatic nucleophilic substitution with benzylamine[38] and subsequent deprotection of the amine[39] yielded both methyl and ethyl esters of 6-amino-5-cyano-2-methylpyridine-3-carboxylic acids **7** and **8** in good yields from commercial materials (Scheme 1). Next, Friedländer reaction[40] with the corresponding cycloalkanone, under standard conditions ($AlCl_3$, 1,2-dichloroethane, reflux)[27] provided compounds **9**−**16** with the desired 1,8-naphthyridine structure (Scheme 2), with yields from medium to excellent. These molecules have been conveniently characterized by their analytical and NMR spectroscopic data.

Biology. AChE/BuChE Inhibitory Activity. Compounds **9**−**16** were evaluated as inhibitors of AChE from both *Electrophorus electricus* (eeAChE) and human erythrocytes (hAChE) and of BuChE from equine serum, following Ellman's method[41] (Table 1). Compared to the eeAChE inhibitory activity of related compounds,[34] compounds **9**−**16** were at least 10-fold more potent than those bearing an aryl substituent at C4, confirming our hypothesis that aryl substituents at C4 were barely accommodated into the catalytic binding site of AChE.[34] Thus, from a previous molecular modeling study with **17**[34] and the X-ray structure of eeAChE,[42] we propose compound **14** could be well-accommodated between Trp86 and Tyr337 of eeAChE, generating a $\pi-\pi$ stacking interaction. This conformation would be facilitated by a hydrogen bond between protonated aromatic nitrogen and the carbonyl group of His447. In agreement with previous studies from our laboratory,[27,34] the cyclohexene moiety was the hit for an optimal inhibition of eeAChE. Replacement of the ethyl by a methyl ester slightly modified the eeAChE inhibitory activity, either improving or lowering the inhibitory activity of eeAChE (Table 1). Inhibition experiments using hAChE showed IC_{50} data in the micromolar range, between 1 and 2.1 μM, except for the cyclohexane-fused ethyl ester derivative **14**, which inhibited hAChE with an IC_{50} of 0.78 μM. It is interesting to note how the cycloalkane ring expansion or contraction diminished the inhibitory activity by approximately 2-fold (Table 1). The reason for the enzymatic selectivity of these compounds, about 10-fold more active eeAChEI than hAChEI, could be due to some structural

Scheme 1. Synthesis of Naphthyridine Precursors[a]

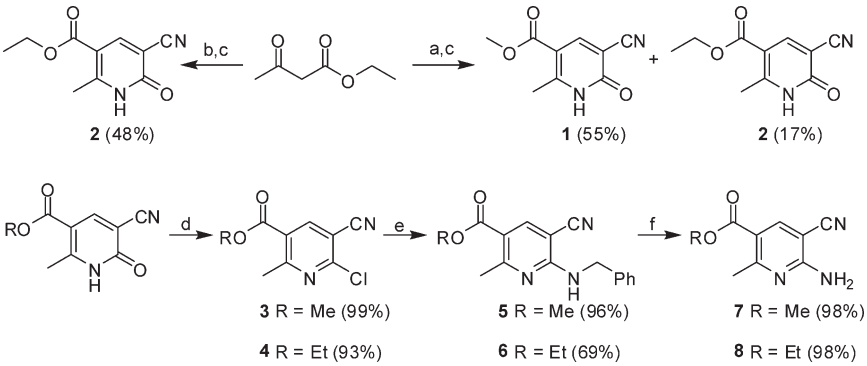

[a] Reagents and conditions: (a) $Me_2NCH(OMe)_2$, DMF, room temp, 24 h; (b) $Me_2NCH(OEt)_2$, DMF, room temp, 24 h; (c) NH_2COCH_2CN, NaH, DMF, room temp, 24 h; (d) $POCl_3$, reflux, 48 h; (e) benzylamine, MeOH, room temp, 4 days; (f) CF_3SO_3H, CH_2Cl_2, reflux, 2 h.

Scheme 2. Synthesis of the 1,8-Naphthyridine Derivatives **9**−**16**

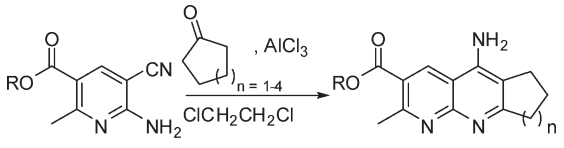

9 R = Me, n = 1 (60%)
10 R = Me, n = 2 (70%)
11 R = Me, n = 3 (67%)
12 R = Me, n = 4 (57%)
13 R = Et, n = 1 (69%)
14 R = Et, n = 2 (93%)
15 R = Et, n = 3 (80%)
16 R = Et, n = 4 (90%)

differences, such as eeAChE being a flexible tetramer,[42] while human erythrocyte AChE is presented in globular dimers,[43] or because they show different rate of glycosylation.[44] Although some authors have not found any differences in the catalytic behavior of both enzymes,[45] there are several papers describing a differential inhibitory activity for eeAChE and human erythrocytes AChE with physostigmine, organophosphorus, and carbamate analogues.[46,47] Otherwise, the fact that these compounds were better inhibitors of eeAChE, an enzyme structurally related to the brain enzyme,[48] than the peripheral human erythrocyte AChE could be beneficial for a potential further clinical development, taking into account that many of the side effects of AChE inhibitors are due to the inhibition of the peripheral enzyme.

Inhibition of eqBuChE by compounds **9**−**16** showed IC_{50} values in a wide concentration range, between 0.49 and 36 μM (Table 1). Fixing the cycloalkane, methyl esters were better BuChEI than ethyl esters. Thus, cycloheptane-fused derivatives **11** and **15** appeared to be the best inhibitors, with IC_{50} of 0.49 and 2.1 μM, respectively. This result could be explained by the fact that BuChE possesses a more open catalytic site. In this manner, ring expansion improved the inhibitory activity because of a better accommodation of cycloheptane-fused derivatives into the catalytic site of BuChE. Compound **11**, the most potent BuChE inhibitor, was 100-fold less potent than tacrine. Also, it was 1.7-fold and 24-fold more potent than donepezil and galantamine, respectively (Table 1). Thus, the potencies to inhibit BuChE were in the order tacrine > compound **11** > donepezil > galantamine. In spite of the lesser potency of these 1,8-naphthyridines compared to tacrine, it is worth noting that compounds **9**−**16** had better activities than 4-aryl-substituted naphthyridine derivatives previously synthesized in our laboratory.[34] The poor inhibitory activity of BuChE found in previously described compounds could be a consequence of discarding either methyl ester or cycloheptene-fused derivatives in the chemical design of our tacrine−1,4-DHP hybrid compounds.

Kinetic Study of AChE Inhibition. The mechanism involved in the AChE inhibition by compounds **9**−**16** was investigated using compound **14**, the most potent AChE inhibitor here described (Table 1). The type of inhibition was elucidated from the analysis of Lineweaver−Burk reciprocal plots (Figure 1) showing both increasing slopes (lower V_{max}) and intercepts (higher K_m) with higher inhibitory concentration. This suggests a mixed-type inhibition.[49] The graphical analysis of steady-state inhibition data for compound **14** is shown in Figure 1. A K_i value of 24 ± 3 nM was estimated from the slopes of double reciprocal plots versus compound **14** concentrations (Figure 1, inset).

Propidium Iodide Displacement Assay. Compounds **9**−**16** were designed to improve their binding to the AChE catalytic site. To confirm whether our compounds could partially interact with the PAS of AChE, experiments to evaluate the competition with propidium iodide for its binding to this site were performed. Propidium, a selective ligand for the PAS of AChE, exhibits a fluorescence increase upon binding to this site.[50] Decrease of propidium fluorescence in the presence of the compounds can be interpreted as a displacement of propidium from the PAS. At 1 and 10 μM, compounds **9**−**16** did not show a significant ability to displace propidium from the PAS of AChE (see Supporting Information). At 10 μM, although compound **10** reduced propidium iodide binding by 16%, it seems that compounds **9**−**16** would preferentially bind to the catalytic binding site rather than to the PAS of AChE.

Effects of Compounds 9−16 on Ca^{2+} Entry Elicited by K^+ Depolarization of SH-SY5Y Cells. Since Ca^{2+} ions are involved in neuronal death in AD,[51] we first studied whether compounds **9**−**16** had any effect on Ca^{2+} entry induced by K^+ depolarization in Fluo-4/AM-loaded SH-SY5Y human neuroblastoma cells. Cells were incubated in the presence of compounds **9**−**16** at 1 μM for 10 min and then stimulated with a concentrated solution of KCl so that the final K^+ concentration in the medium was 70 mM. At 3 μM, the 1,4-DHP nifedipine caused 46% inhibition of K^+-evoked $[Ca^{2+}]_c$ increase. Most compounds had no effect on Ca^{2+} uptake (see Supporting Information). Only compound **12** significantly blocked Ca^{2+}

Table 1. Inhibition of AChE from both *Electrophorus electricus* (eeAChE) and Human Erythrocytes (hAChE) and of BuChE from Equine Serum (eqBuChE) by 1,8-Naphthyridines **9**−**16**

		IC_{50} (μM)[a]			
compd	R, *n*	eeAChE	eqBuChE	hAChE	selectivity eqBuChE/eeAChE
tacrine		0.027 ± 0.002	0.0052 ± 0.0002	0.10 ± 0.01	0.193
donepezil		0.0134 ± 0.0009	0.84 ± 0.05	0.0082 ± 0.0004	62.7
galantamine		0.56 ± 0.06	12 ± 1	0.60 ± 0.04	21.4
9	R = Me, *n* = 1	0.12 ± 0.01	5 ± 1	1.9 ± 0.2	41.7
10	R = Me, *n* = 2	0.093 ± 0.005	3.4 ± 0.3	1.0 ± 0.1	36.6
11	R = Me, *n* = 3	0.36 ± 0.07	0.49 ± 0.03	2.0 ± 0.3	1.36
12	R = Me, *n* = 4	0.25 ± 0.03	4.07 ± 0.07	1.8 ± 0.2	16.3
13	R = Et, *n* = 1	0.35 ± 0.04	39 ± 7	2.1 ± 0.2	111
14	R = Et, *n* = 2	0.060 ± 0.006	12 ± 1	0.78 ± 0.08	200
15	R = Et, *n* = 3	0.31 ± 0.02	2.1 ± 0.2	2.0 ± 0.3	6.77
16	R = Et, *n* = 4	0.40 ± 0.02	5.3 ± 0.3	1.8 ± 0.2	13.2
17[34]		0.8 ± 0.2	5.0 ± 0.6		6.1

[a] IC_{50} values are the mean ± SEM of quadruplicates of at least three independent experiments.

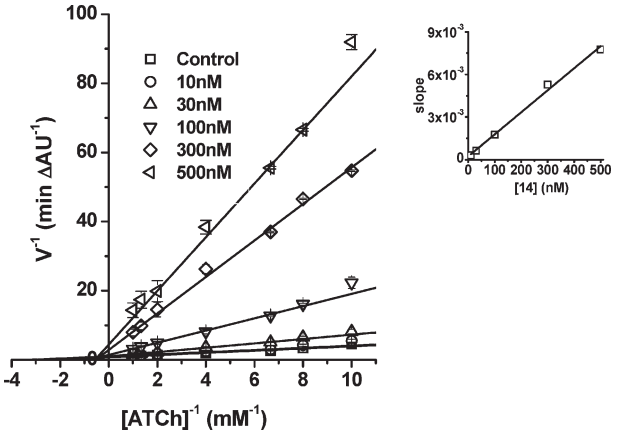

Figure 1. Steady-state inhibition of AChE hydrolysis of acetylthiocholine (ATCh) by compound **14**. Lineweaver−Burk reciprocal plots of initial velocity and substrate concentrations (0.1−1 mM) are presented. Lines were derived from a weighted least-squares analysis of data. Inset: slope of the double reciprocal plots versus [**14**].

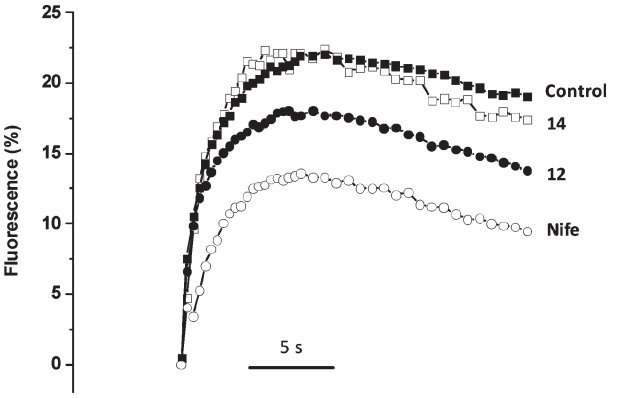

Figure 2. Effect of compounds **12** and **14** on $[Ca^{2+}]_c$ increase induced by high K^+ in SH-SY5Y neuroblastoma cells. Experiments were performed in Fluo-4-loaded cells (n = 4). The curves are representative examples of the averaged time course of $[Ca^{2+}]_c$ in control conditions and in the presence of **12**, **14** (at 1 μM), or nifedipine at 3 μM.

entry by 20% (Figure 2). Figure 2 also shows the time course of $[Ca^{2+}]_c$ changes in cells treated with nifedipine or with compound **14**, as an example of those compounds unable to inhibit $[Ca^{2+}]_c$ increases. The absence of Ca^{2+} channel regulatory activity of these new compounds in comparison to previous analogues was expected, since the 1,4-DHP moiety, which is believed to confer such activity, is absent.[26,34] As shown in Chart 2, substituent X used to be an aryl ring, while it is a hydrogen in compounds **9**−**16**. Hence, they are not tacrine-1,4-DHP hybrids any longer.

Effects of Compounds 9−16 on Cell Viability. Before evaluating the neuroprotective properties of these compounds, we tested whether compounds **9**−**16** exerted cytotoxic effects by themselves in human SH-SY5Y neuroblastoma cell line by measuring lactate dehydrogenese (LDH) release as a parameter of cell death. All compounds were studied by incubation of cells with compounds at 1 μM for 24 h. In all cases, LDH release was not statistically significant with respect to the DMSO group. Therefore, compounds **9**−**16** were not toxic at the concentration we are using to analyze their neuroprotective effects (see Supporting Information).

Neuroprotective Effect of Compounds 9−16 against Rotenone/Oligomycin A Induced Cell Death. Rotenone and oligomycin A block complexes **I** and **V**, respectively, of the mitochondrial electron transport chain, thus disrupting ATP synthesis.[52] The exposure of SH-SY5Y cells to a mixture of rotenone plus oligomycin A (Rot/Olig) constitutes a good model of oxidative stress having its origin in mitochondria; it elicits neurotoxicity and allows the evaluation of potential neuroprotective drugs used to treat AD patients, which inhibit AChE, such as galantamine, donepezil, and rivastigmine. Hence, the neuroprotective effect of compounds **9**−**16** against this toxic stimulus was evaluated with the method of the LDH release[53] at 1 μM on SH-SY5Y neuroblastoma cells, exposed to 30 μM rotenone plus 10 μM oligomycin-A for 24 h. The results, shown in Figure 3, indicate that these compounds efficiently protected against oxidative stress in the same range as well-known reference antioxidants such as melatonin (MEL) and *N*-acetylcysteine (NAC).[54] Most of the compounds produced approximately a 30% decrease in cell death induced by Rot/Olig (Figure 3 and Supporting Information). Compounds **12** and **14** reduced cell death by 42% and 48%, respectively, while 4-phenyl-substituted analogue **17** protected by 27% (Figure 3). The good profile of these compounds as neuroprotectants against Rot/Olig neurotoxicity is currently an open question that deserves further studies.

Effect of Compounds 9−16 on Okadaic Acid Induced Cytotoxicity. Okadaic acid (OA), a potent and nonselective inhibitor of Ser/Thr phosphatases, induces τ hyperphosphorylation and cell death in both primary cortical neurons

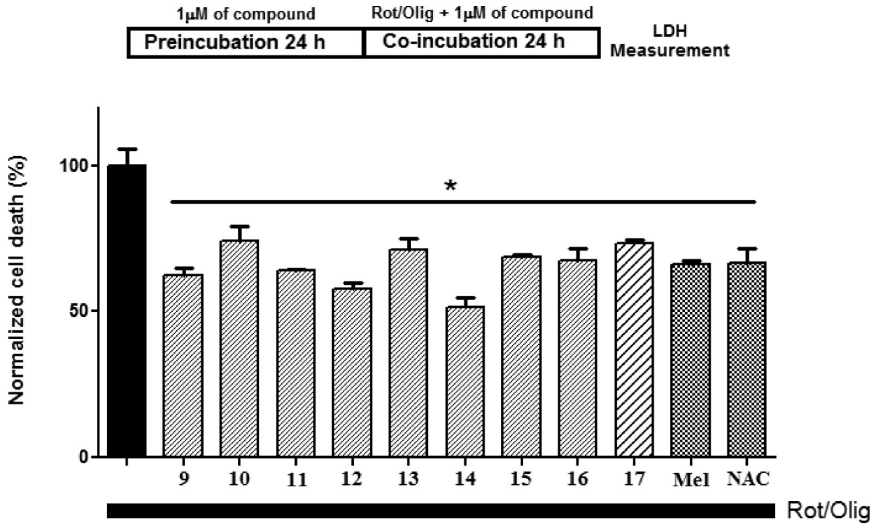

Figure 3. LDH release assay with rotenone/oligomycin A stimulated SH-SY5Y cells in the presence of compounds **9**−**16** or the 4-phenyl-substituted analogue **17**. SH-SY5Y neuroblastoma cells were treated with 1 μM drugs 24 h before and during the incubation period with the toxic stimulus (30 μM rotenone plus 10 μM oligomycin-A, Rot/Olig). The 10 nM melatonin (Mel) and 1 mM *N*-acetylcysteine (NAC) were used as reference compounds. After exposure to Rot/Olig, cell death was quantified by measuring the LDH released to the media and normalized in each individual experiment as percentage with respect to the maximum LDH released, considered as 100% cell death, and LDH released by nontreated cells, considered as 0% cell death. Data are the means ± SEM of triplicates of seven different cell batches: (*) $p < 0.05$ in comparison to control cell death.

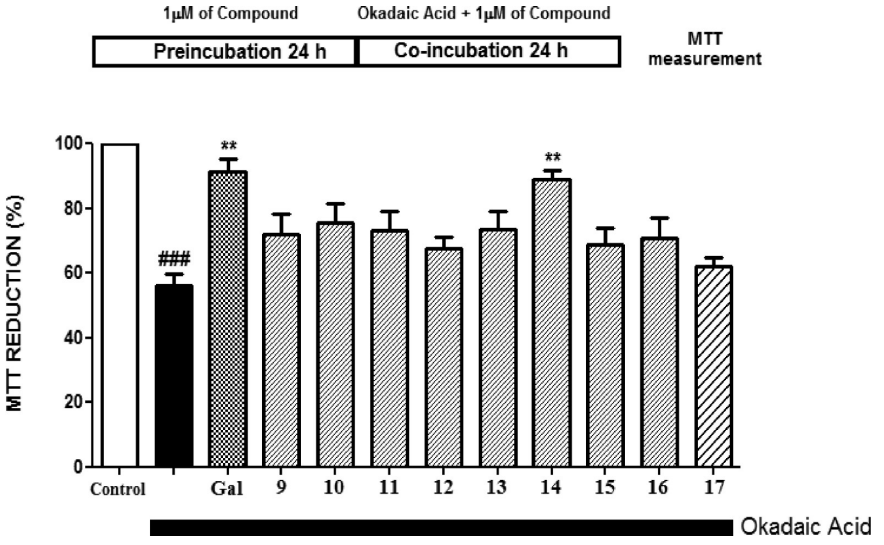

Figure 4. MTT reduction assay in okadaic acid stimulated SH-SY5Y cells in the presence of compounds **9**−**16** and the 4-phenyl-substituted analogue **17**. SH-SY5Y neuroblastoma cells were treated with 1 μM compounds or 0.3 μM galantamine (used as reference compound) 24 h before and during the incubation period with the toxic stimulus (30 nM okadaic acid, 24 h). After this period, cell viability was quantified by evaluating MTT reduction to a formazan salt. Control group was considered as 100% of viability and represents cell viability of cells incubated only with cell culture medium. Data are the mean ± SEM of triplicates of seven different cell batches: (###) $p < 0.001$, comparing control and okadaic acid-lesioned cells; (**) $p < 0.01$, comparing to okadaic acid lesioned cells in the absence of drug.

and neuroblastoma cell lines, which leads to subsequent neuronal degeneration, synaptic loss, and memory impairment, resembling AD pathology.[55,56] Although these experimental paradigms are insufficient to characterize the development of AD pathology, they provide a potentially useful tool for determining the role of τ hyperphosphorylation in neuronal death processes.[55,56] In this study, SH-SY5Y cells were incubated with compounds **9**−**16** at 1 μM for 24 h before addition of 30 nM OA and co-incubated with OA and the selected compound for an additional 24 h period. Cell viability at the end of this period was evaluated by the MTT reduction method,[57] as described in the Experimental Section. Results are expressed as percentage of MTT reduction with respect to nontreated (control) cells; this value was taken as 100% of cell viability. Galantamine (GAL), at 0.3 μM, was used as reference.[58] Compound **17** did not protect SH-SY5Y cells against OA. Only compound **14** protected cells against OA-induced cell death with statistically significant values. Cells treated with compound **14** were able to reduce MTT by 89% compared to control, having 75% more viability than that found in OA cells. MTT was reduced by 91% compared to control in cells incubated with OA plus GAL. Thus, by comparison to OA cells, GAL afforded 85% protection against OA-elicited toxicity (Figure 4).

Molecular Modeling Studies on Okadaic Acid Induced Toxicity Prevention by Compound 14. Molecular field-based similarity is a powerful tool for identifying patterns in bioactive molecules, even when the molecules appear quite

Scheme 3. Tautomeric Equilibrium for Compound **14**

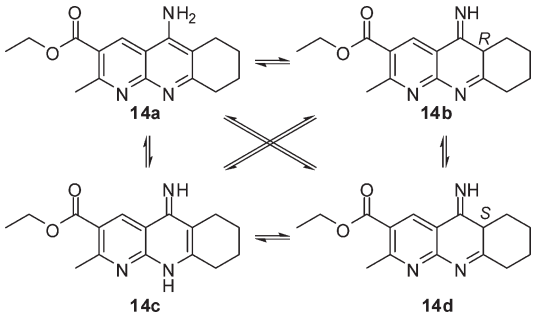

Chart 3. Structure of Okadaic Acid and Tautomer **14d** Showing the Regions and the Selected Atoms To Be Aligned

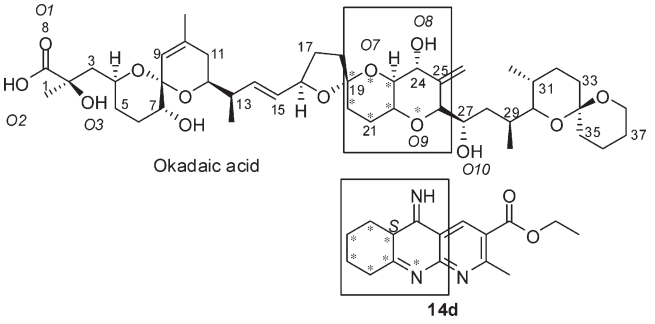

dissimilar. To locate the structural commonalities, molecules must be superimposed with respect to their molecular field (steric, electrostatic, etc.). In some cases many possible superpositions of nearly equal similarity can exist; therefore, it is essential that consistent superimpositions be obtained through the use of higher-order similarity relations.

In order to understand the good biological data of compound **14** protecting SH-SY5Y neuroblastoma cells against cell death elicited by OA-induced τ hyperphosphorylation, molecular modeling studies of these two structurally different molecules have been done. We used OA as the 3D template to locate essential features for recognition of ligands that bind to the same receptor. Compound **14** might exist in amino and imino tautomeric forms, and it is noted that in tautomers **14b** and **14d** there is a chiral center (Scheme 3).

When OA and compound **14** were compared, a location in OA that has two regions to fit with compound **14** was found. OA and each of the four tautomers were compared for stereoelectronic congruence on the basis of cyclohexane and aminopyridine rings attachment onto the two tetrahydropyran rings (Chart 3). The quantitative criterion used for judging the superimposition of the ligands and template is the root means square (rms) distance between selected atoms in the ligand and the paired atoms of the template. The selected atoms are the ones marked by an asterisk in Chart 3. Tautomer **14d**, with *S* configuration, showed the best fit with a rms deviation of 0.188 Å.

The structural similarities between tautomer **14d** and OA are depicted in Figure 5, where a rigid least-squares fit has been performed. The structural congruences between the cyclohexane and the tetrahydropyran rings, and the aminopyridine ring with the other tetrahydropyran ring are evident from the Figure 5. Moreover, the imino group and two pyridine nitrogens in compound **14d** are in the same region as O8, O9, and O10 (Chart 3 and Figure 5) in OA, respectively.

To assess the electronic congruence between these two molecules, we have calculated their electrostatic potential

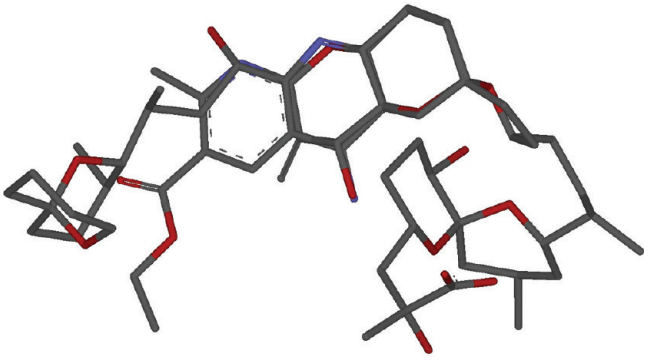

Figure 5. Superposition of tautomer **14d** and okadaic acid. Hydrogen atoms are omitted for clarity.

surfaces (EPS) and performed a similarity analysis in the same way as before (Figure 6).

At the top of each compound we can recognize a red area corresponding to a region of high electronic density; the same occurs in the region of the imino group (**14d**) and O8 (OA). Therefore, tautomer **14d** and OA are congruent in an electrostatic sense in these areas, which can play an important role for the binding to the receptor. On the basis of the molecular modeling studies, we propose that the active conformation of compound **14** is the tautomer **14d.**

Reduction of the OA-Induced PP2A Inhibition by Compound 14. According to the molecular modeling studies, compound **14** would be competing with OA for the binding to Ser/Thr phosphatases, e.g., PP2A, preventing OA-induced phosphatases inhibition. Since compound **14** would be mimicking a portion of OA not essential for its inhibitory activity, the entry of OA to the binding site would be hampered, but Ser/Thr phosphatase-catalyzed τ dephosphorylation would be preserved. PP2A is the most OA-sensitive Ser/Thr phosphatase enzyme.[59] To confirm this hypothesis, experiments of PP2A inhibition with OA in the presence of compound **14** were carried out by the method of the malachite green (Figure 7).[60,61] Immunoprecipitated PP2A was able to release 1.90 ± 0.07 nmol ($100 \pm 4\%$ control) of inorganic phosphorus to the assay medium. This phosphate generation was significantly reduced in the presence of 30 nM OA (1.31 ± 0.01 nmol, $69 \pm 2\%$ control). Under these experimental conditions, compound **14** significantly prevented the OA inhibitory activity in a concentration-dependent manner. At 1 μM and in the presence of 30 nM OA, compound **14** increased the inorganic phosphorus release to 1.456 ± 0.004 nmol ($77 \pm 2\%$ control). This effect was more significant when the concentration of compound **14** was 10 μM, generating 1.72 ± 0.01 nmol of inorganic phosphorus ($91 \pm 3\%$ control) (Figure 7).

Molecular Docking of Compound 14 with PP2A. In order to go into depth into the binding mode of compound **14** compared to OA in PP2A, a molecular docking analysis has been carried out. The blind docking of the **14d**−PP2A molecules was successful as indicated by the statistically significant scores. An important finding is the location of the binding site, which is situated where we proposed based on superimposition protocol (Figure 8).

Figure 9 shows the residues involved in the predicted binding site. Hydrogen bond interaction of the ester side chain with Arg214 may strengthen the ligand binding.

Thus, the computational studies were in accordance with the biological activity found for compound **14**, with regard to

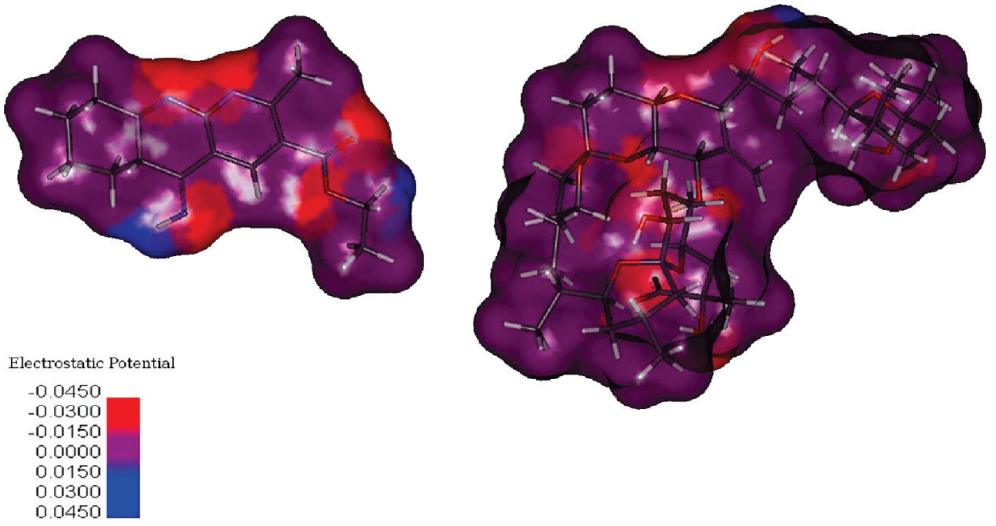

Figure 6. Molecular electrostatic potential surfaces for tautomer **14d** (left) and okadaic acid (right).

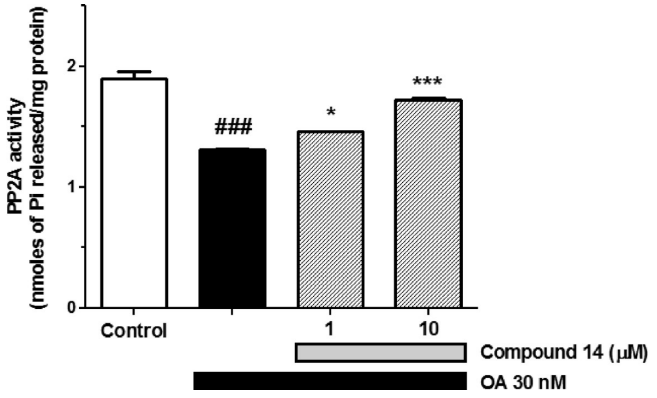

Figure 7. Effect of compound **14** on the inhibition of PP2A-derived phosphatase activity induced by OA, measured with the malachite green assay. Immunoprecipitated PP2A from rat brain lysates was treated with vehicle (control), 30 nM OA (maximal inhibition), and 30 nM OA plus **14** (1 or 10 μM), before adding the threonine phosphopeptide (Lys-Arg-pThr-Ile-Arg-Arg) used as enzymatic substrate. After 10 min, malachite green was added and the enzymatic reaction was allowed 15 min more for color development. After this period, PP2A activity was quantified by measuring color generation at 620 nm. Control group represents the maximal phosphatase activity. Data are the mean ± SEM of triplicates of two different brain lysates: (###) $p <$ 0.001 versus control; (*) $p < 0.05$ and (***) $p < 0.001$ in comparison to OA in the absence of drug.

the prevention of OA-induced inhibition of PP2A. Hence, the neuroprotective activity induced by compound **14** against the toxicity elicited by OA (Figure 4) was hypothesized to be due to this down-regulating effect of the OA-induced Ser/Thr phosphatases inhibition.

Neuroprotection of Compound 14 against Aβ-Induced Cytotoxicity. Taking into account the good neuroprotective profile of compound **14** against models of both τ hyperphosphorylation and oxidative stress, we evaluated whether it was also able to protect against the neurotoxicity evoked by Aβ_{1-42}. The 1−42 peptide is the most amyloidogenic isoform of Aβ.[62] When SH-SY5Y neuroblastoma cells were exposed to 30 μM Aβ_{1-42} for 24 h, cell viability, measured as MTT reduction, decreased significantly (78 ± 2% vs control; Figure 10). We found that compound **14** was able to increase cell viability in a concentration-dependent manner (0.1−1 μM). When cells were treated with Aβ_{1-42} plus compound **14** at 1 μM for 24 h, viability augmented significantly to 90 ± 1%, which implies 54% more viability than that found in cells treated only with exogenous Aβ_{1-42}. Used as reference compound, 10 nM melatonin caused 58% protection.[63,64]

Neuroprotection Elicited by Compound 14 in Rat Hippocampal Slices Subjected to Oxygen and Glucose Deprivation. Because compound **14** exhibited neuroprotective properties against different stressors in neuroblastoma cell cultures, it was of interest to test whether the compound exerted neuroprotection in a more complex model, e.g., the rat hippocampal slice subjected to oxygen and glucose deprivation (OGD) followed by reoxygenation. Thus, 15 min of OGD followed by 2 h reoxygenation produced 35% decrease of cell viability with respect to control slices. We found that compound **14** was able to increase cell viability in a concentration-dependent manner (1−30 μM), with a maximal protection of 65.5% at 30 μM. This protection was comparable to that of the reference drug galantamine.[65] EC_{50} for compound **14** was 6 μM (Figure 11).

Conclusions

We have synthesized and evaluated a series of 1,8-naphthyridine derivatives related to tacrine and compound **17**, a neuroprotectant previously reported by our research group. These new compounds were easily prepared by smooth reactions in high yields from readily available precursors. The compounds were dual inhibitors of both AChE and BuChE, with slight selectivity toward AChE inhibition. Cholinesterase inhibition was modulated by tiny modifications of the structure. AChE inhibition was improved in cyclohexene-fused compounds, while BuChE inhibition was better in methyl esters than in ethyl esters, the cycloheptene-fused compound **11** being the most active. Compared to previous 1,8-naphthyridines reported by our group, removal of the aryl susbtituent at C4 improved both AChE and BuChE inhibition. Only compound **12** kept the Ca^{2+} channel modulating activity (20% blockade) as found in previously described compounds. Furthermore, these 1,8-naphthyridine derivatives showed neuroprotection against oxidative stress elicited by the rotenone/oligomycin A cocktail, but only compound **14**, the best AChE inhibitor of this series, was able to improve cell viability of SH-SY5Y cells subjected to OA-induced τ hyperphosphorylation. Also, compound **14** protected SH-SY5Y cells

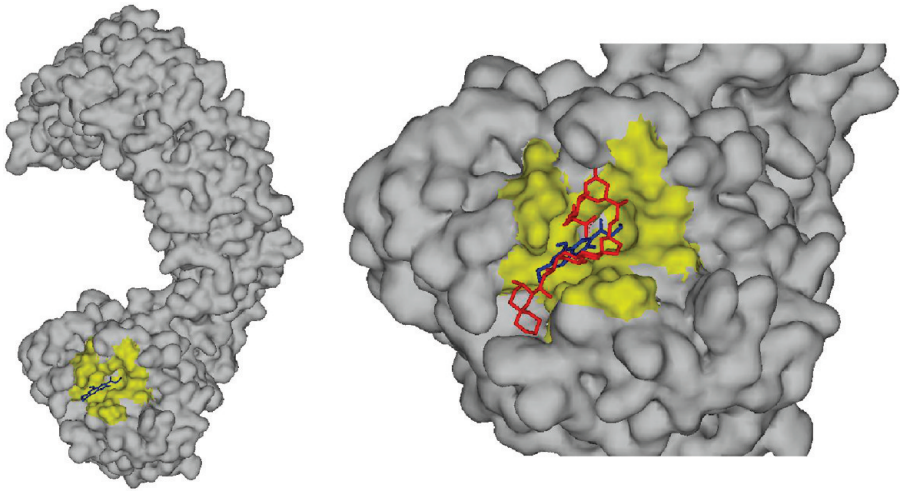

Figure 8. (a, left) Molecular docking model of **14d**−PP2A complex. Yellow portions indicate positions of the pocket. (b, right) Molecular docking model of **14d**−PP2A complex including okadaic acid (zoom): **14d** (blue), okadaic acid (red).

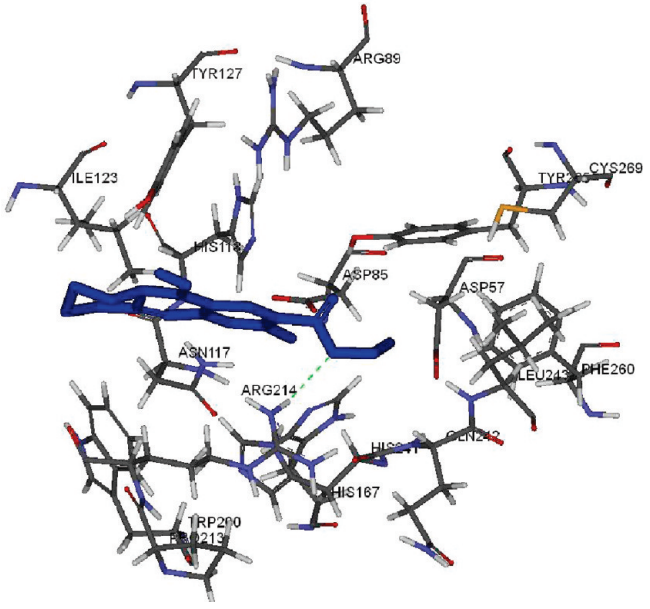

Figure 9. Binding mode of the most stable docked orientation of **14d** with PP2A.

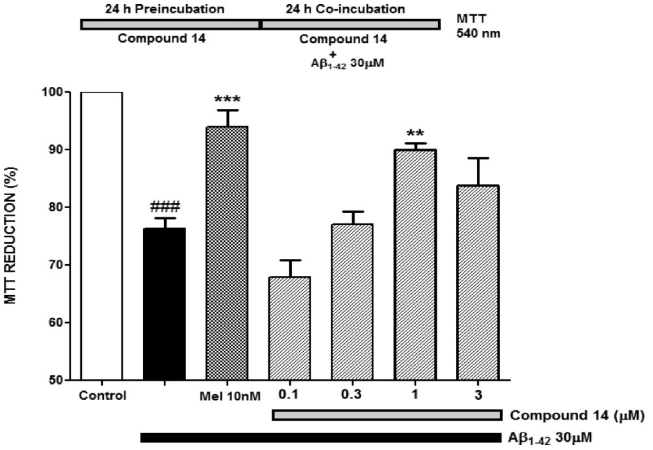

Figure 10. MTT reduction assay in Aβ-lesioned SH-SY5Y neuroblastoma cells in the presence of compound **14**. Neuroblastoma cells were treated with **14** (0.1−3 μM) or 10 nM of melatonin (Mel, used as reference) 24 h before and during a 24 h incubation period with 30 μM Aβ_{1-42}. After this period, cell viability was quantified by measuring MTT reduction. Control group was considered as 100% and represents cell viability of cells incubated only in culture medium. Data are the mean ± SEM of triplicates of four different cell batches: (##) $p < 0.01$ versus control; (**) $p < 0.01$ and (***) $p < 0.001$ in comparison to Aβ_{1-42} lesioned cells in the absence of drug.

against Aβ_{1-42} neurotoxicity in concentration-dependent manner. On the basis of this promising neuroprotective profile, compound **14** was studied in an experimental preparation that mimics tissue neurodegeneration, the rat hippocampal slices subjected to OGD and reoxygenation, where it protected up to 65.5% against this toxic stimulus, with an EC_{50} of 6 μM. As this family of 1,8-naphthyridines scarcely affected Ca^{2+} entry, they should exert their neuroprotective actions by a different mechanism, e.g., free radical scavenging. This would explain the neuroprotective profile of compound **14** in the OGD experiments, as well as Rot/Olig experiments. The fact that compound **14** also offered neuroprotection against both OA-induced τ hyperphosphorylation and exposure to exogenous Aβ makes us think that its mechanism of action could be located at the beginning of the cascade of events that lead to neurodegeneration. Likely, as hypothesized by computational studies, compound **14** could be preventing the Ser/Thr phosphatase inhibition. The maintenance of the Ser/Thr phosphatase activity exerted by compound **14** could have consequences in a neurodegeneration scenario, reducing the generation of neurofibrilary tangles by slowing down the τ hyperphosphorylation. Hence, compound **14** improves the neuroprotective properties of previous neuroprotectants described by our group, like compound **17**. For these reasons, compound **14** (ethyl 4-amino-2-methyl-6,7,8,9-tetrahydrobenzo[*b*][1,8]naphthyridine-3-carboxylate) can be considered as a new potential neuroprotective drug acting on different models of neurodegeneration, both in neuroblastoma cultures and in cerebral tissues, which deserves a further preclinical investigation and characterization of its mechanism of action. Together with compound **14**, compound **12** also presented interesting properties, since it exhibited moderate and dual inhibitory activity of cholinesterases (IC_{50} of 0.25 and 4.07 μM to inhibit eeAChE and eqBuChE, respectively), K^+-evoked Ca^{2+} entry blockade, and a 42% protection of SH-SY5Y neuroblastoma cell line against rotenone/oligomycin A neurotoxicity. This pharmacological profile could be interesting taking into account that Ca^{2+} channel blockade

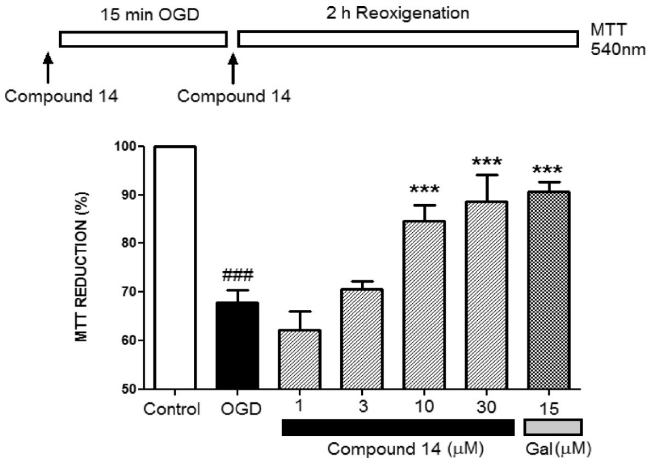

Figure 11. MTT reduction assay in rat hippocampal slices subjected to 15 min of OGD and 120 min of reoxygenation in absence (OGD bar) or presence of increasing concentrations (1, 3, 10, and 30 μM) of compound **14** (see protocol at the top of the figure). Galantamine (GAL, 15 μM) was used as reference. Slices, kept during the same period of time with oxygen and glucose, were run in parallel to define the control condition (Control). MTT reduction in control slices was taken as 100% of tissue viability. Data are the mean ± SEM of six experiments: (###) $p < 0.001$ comparing control respect to OGD; (***) $p < 0.001$ in comparison to OGD.

has been reported to induce neuroprotection in several models of cell death.[32,33] The results of this work are in agreement with the current opinion about the necessity of finding multitarget drugs for the development of AD medicines, like dimebon,[66] an antihistaminic and anticholinesterasic drug that was found to preserve mitochondrial function[67] and protected neurons against several neurotoxic stimuli.[68]

Experimental Section

Materials. Melatonin, rotenone, oligomycin A, *N*-acetylcysteine (NAC), tacrine, nifedipine, dimethyl sulfoxide (DMSO), EDTA, EGTA, leupeptin, PMSF, Aβ protein fragment 1−42, and okadaic acid were purchased from Sigma Aldrich (Madrid, Spain). Galantamine was purchased from Tocris House (Bristol, U.K.). Protease inhibitor cocktail was purchased from Roche (Mannheim, Germany). Fluo-4/AM was purchased from Molecular Probes (Invitrogen, Barcelona, Spain), and PP2A immunoprecipitation phosphatase assay kit was purchased from Millipore (Temecula, CA).

Chemistry. Reactions were monitored by TLC (thin layer chromatography) using precoated silica gel aluminum plates containing a fluorescent indicator. Detection was done by UV (254 nm) followed by charring with sulfuric−acetic acid spray, 1%, aqueous potassium permanganate solution, or 0.5% phosphomolybdic acid in 95% ethanol. Anhydrous Na_2SO_4 was used to dry organic solutions during workups, and the removal of solvents was carried out under vacuum with a rotary evaporator. Flash column chromatography was performed using silica gel 60 (230−400 mesh). Melting points were determined in a Stuart SMP-10 apparatus and are uncorrected. IR spectra were obtained in a Bruker IFS60v spectrophotometer. MS spectra were obtained in a QSTAR spectrometer (Applied Biosystems). ^{1}H and ^{13}C NMR spectra were recorded with a Varian VXR-200S or Bruker AMX-300 spectrometer, using tetramethylsilane as internal standard. All the assignments for protons and carbons were in agreement with 2D COSY, gHSQC, gHMBC, and 1D NOESY spectra. Elemental analyses were used to determine the purity of compounds and carried out on a LECO CHNS-932 apparatus. Positive electrospray HRMS spectra were obtained in an API QSTAR pulsar spectrometer (Applied Biosystems). All the described compounds had ≥95% purity.

General Method for the Synthesis of 6(1*H*)-Pyridinone Derivatives. In a three-necked round-bottomed flask, a mixture of the corresponding alkyl acetoacetate (1 equiv) and *N*,*N*′-dimethylformamide dialkyl acetal (1 equiv) in dry DMF (1 mL/mmol) was stirred at room temperature under argon for 24 h. A mixture of cyanoacetamide (1 equiv) and sodium hydride (2 equiv) in dry DMF (1.4 mL/mmol), previously prepared at 0 °C and stirred at room temperature for 10 min under argon, was added slowly, and the mixture was allowed to stir for 24 h. A solution of ethanol/H_2O (50:50, 5 mL/mmol) was added, and the resulting mixture was acidified to pH 4 with concentrated HCl and stirred for 24 h. The mixture was filtered to afford a solid with good analytical and spectral data.

Methyl Ester of 5-Cyano-2-methyl-6-oxo-1,6-dihydropyridine-3-carboxylic Acid (1). Following the general method for the synthesis of 2(1*H*)-pyridinone derivatives, reaction of ethyl acetoacetate (6.500 g, 50 mmol) and *N*,*N*′-dimethylformamide dimethyl acetal (5.950 g, 50 mmol) in dry DMF (50 mL) afforded after filtration a yellow solid that was assigned to compound **1** (5.280 g, 55%) with spectral data in accordance with the literature.[36] Anal. ($C_9H_8N_2O_3$) C, H, N.

Ethyl Ester of 5-Cyano-2-methyl-6-oxo-1,6-dihydropyridine-3-carboxylic Acid (2). Following the general method for the synthesis of 2(1*H*)-pyridinone derivatives, reaction of ethyl acetoacetate (3.797 g, 29.2 mmol) and *N*,*N*′-dimethylformamide diethyl acetal (4.295 g, 29.2 mmol) in dry DMF (29 mL) afforded after filtration a yellow solid that was assigned to compound **2** (2.900 g, 48%) with spectral data in accordance with the literature.[36] Anal. ($C_{10}H_{10}N_2O_3$) C, H, N.

General Method for the Synthesis of 6-Chloropyridine Derivatives. The corresponding 6(1*H*)-pyridinone was dissolved in $POCl_3$, and the mixture was heated under reflux. Ice (40−80 g) was poured into the mixture, and the mixture was neutralized (pH 7) with aqueous ammonia. The resulting solid was filtered and washed with H_2O. Pure compounds were isolated after desiccation with a vacuum pump.

Methyl Ester of 6-Chloro-5-cyano-2-methylnicotinic Acid (3). Following the general method for the synthesis of 6-chloropyridine derivatives, reaction of **1** (1.000 g, 5.20 mmol) in $POCl_3$ (10 mL), after 41 h, yielded compound **3** (1.085 g, 99%) as a yellow solid. IR (KBr) ν 3431, 3074, 2925, 2854, 2238, 1727, 1588, 1535, 1437, 1416, 1282, 1245, 1113, 929, 782 cm^{-1}; ^{1}H NMR ($CDCl_3$, 300 MHz) δ 8.39 (s, 1 H, H4), 3.88 (s, 3 H, OCH_3), 2.81 [s, 3 H, CH_3(C2)]; ^{13}C NMR ($CDCl_3$, 75.4 MHz) δ 165.7 (C6), 164.6 (CO), 154.3 (C2), 145.1 (C4), 124.7 (C3), 114.5 (CN), 108.6 (C5), 53.4 (OCH_3), 25.6 [CH_3(C2)]. MS (API-ES+) m/z: $[M + 1]^+$ 211.0.

Ethyl Ester of 6-Chloro-5-cyano-2-methylnicotinic Acid (4). Following the general method for the synthesis of 6-chloropyridine derivatives, reaction of **2** (2.000 g, 9.70 mmol) in $POCl_3$ (10 mL), after 48 h, yielded compound **4** (2.023 g, 93%) as a yellow solid. IR (KBr) ν 3431, 3063, 2991, 2926, 2850, 2239, 1723, 1582, 1533, 1413, 1370, 1357, 1275, 1241, 1110, 1033, 988, 872, 782 cm^{-1}; ^{1}H NMR ($CDCl_3$, 300 MHz) δ 8.43 (s, 1 H, H4), 4.35 (q, 2 H, J = 7.1 Hz, $CO_2CH_2CH_3$), 2.80 [s, 3 H, CH_3(C2)], 1.37 (t, 3 H, J = 7.1 Hz, $CO_2CH_2CH_3$); ^{13}C NMR ($CDCl_3$, 75.4 MHz) δ 165.7 (C6), 164.1 (CO), 154.1 (C2), 145.0 (C4), 125.1 (C3), 114.5 (CN), 108.5 (C5), 62.7 ($CO_2CH_2CH_3$), 25.6 [CH_3(C2)], 14.6 ($CO_2CH_2CH_3$). MS (API-ES+) m/z: $[M + 1]^+$ 225.1; $[M + Na]^+$ 247.1.

General Method for the Synthesis of Benzyl-Protected Aminopyridine Derivatives. A mixture of the corresponding 6-chloropyridine (1 equiv) and benzylamine (1−1.2 equiv) in methanol (2 mL/mmol) was stirred at room temperature for several days. The solution was then poured into ice-cold water (10−20 mL/mmol) and kept overnight in a refrigerator. The resulting precipitate was filtered and purified by silica gel flash chromatography using hexane/ethyl acetate mixtures as eluent to give pure compounds.

Methyl Ester of 6-(Benzylamino)-5-cyano-2-methylnicotinic Acid (5). Following the general method for the synthesis of benzyl-protected aminopyridine derivatives, reaction of **3** (506 mg, 2.40 mmol) and benzylamine (309 mg, 2.88 mmol) in MeOH (7 mL), after 7 days, yielded compound **5** (648 mg, 96%) as a white solid. IR (KBr) ν 3354, 3034, 2957, 2223, 1719, 1599, 1580, 1454, 1435, 1325, 1262, 1237, 1210, 1149, 1090, 780, 693 cm^{-1}; ^1H NMR ($CDCl_3$, 300 MHz) δ 8.28 (s, 1 H, H4), 7.35 (m, 5H, Ph), 5.75 (br, 1 H, NH), 4.79 (d, J = 8.7 Hz, 2 H, CH_2), 3.86 (s, 3 H, OCH_3), 2.77 [s, 3 H, CH_3(C2)]; ^{13}C NMR (DMSO-d_6, 75.4 MHz) δ 165.1, 164.9 (CO, C6), 157.8 (C2), 145.2 (C4), 139.5 (C1′), 128.4 (C3′), 127.7 (C2′), 127.0 (C4′), 116.1 (C3), 112.8 (CN), 88.1 (C5), 52.0 (CO_2CH_3), 44.2 (CH_2N), 25.7 [CH_3(C2)]. MS (API-ES+) m/z: $[M + 1]^+$ 282.3, 296.3; $[M + Na]^+$ 304.3, 318.3.

Ethyl Ester of 6-(benzylamino)-5-cyano-2-methylnicotinic Acid (6). Following the general method for the synthesis of benzyl-protected aminopyridine derivatives, reaction of **4** (225 mg, 1.00 mmol) and benzylamine (129 mg, 1.20 mmol) in MeOH (2 mL), after 4 days, yielded compound **6** (203 mg, 69%) as a white solid. IR (KBr) ν 3350, 3062, 3032, 2985, 2926, 2903, 2225, 1716, 1600, 1582, 1454, 1403, 1368, 1327, 1258, 1234, 1148, 1109, 1091, 1033, 779, 742, 714, 693, 615 cm^{-1}; ^1H NMR ($CDCl_3$, 300 MHz) δ 8.29 (s, 1 H, H4), 7.35 (m, 5H, Ph), 5.72 (br, 1 H, NH), 4.79 (d, J = 8.4 Hz, 2 H, CH_2), 4.32 (q, J = 7.2 Hz, 2 H, $CO_2CH_2CH_3$), 2.77 [s, 3 H, CH_3(C2)], 1.37 (t, 3 H, J = 7.2 Hz, $CO_2CH_2CH_3$); ^{13}C NMR ($CDCl_3$, 75.4 MHz) δ 166.5, 165.3 (CO, C6), 158.2 (C2), 144.9 (C4), 138.3 (C1′), 129.2 (C3′), 128.4 (C2′), 128.2 (C4′), 116.6 (C3), 114.7 (CN), 89.1 (C5), 61.3 ($CO_2CH_2CH_3$), 45.7 (CH_2N), 26.4 [CH_3(C2)], 14.7 ($CO_2CH_2CH_3$). MS (API-ES+) m/z: $[M + 1]^+$ 296.0; $[M + Na]^+$ 318.0. Anal. ($C_{17}H_{17}N_3O_2$) C, H, N.

General Method for the Synthesis of Aminopyridine Derivatives. Trifluoromethanesulfonic acid (10−13 equiv) was added dropwise to a solution of the corresponding benzyl-protected 6-aminopyridine in anhydrous dichloromethane (8 mL/mmol) under argon at 0 °C. The mixture was then refluxed for 2−3 h, cooled and diluted in water, basified to pH 10 with 10% NaOH, and extracted with dichloromethane. The organic phase was dried over anhydrous sodium sulfate, evaporated, and purified by flash chromatography using hexane and ethyl acetate mixtures as eluent to give pure compounds.

Methyl Ester of 6-Amino-5-cyano-2-methylnicotinic Acid (7). Following the general method for the synthesis of aminopyridine derivatives, reaction of **5** (69 mg, 0.25 mmol) and trifluoromethanesulfonic acid (482 mg, 3.22 mmol) in dichloromethane (2 mL) after 3 h yielded compound **7** (47 mg, 98%) as a yellow solid. IR (KBr) ν 3387, 3334, 3144, 2224, 1719, 1667, 1598, 1550, 1439, 1340, 1292, 1265, 1170, 1072, 780 cm^{-1}; ^1H NMR ($CDCl_3$, 300 MHz) δ 8.31 (s, 1 H, H4), 5.55 (br, 2 H, NH_2), 3.87 (s, 3 H, OCH_3), 2.73 [s, 3 H, CH_3(C2)]. MS (API-ES+) m/z: $[M + 1]^+$ 192.2; $[M + Na]^+$ 214.0.

Ethyl Ester of 6-Amino-5-cyano-2-methylnicotinic Acid (8). Following the general method for the synthesis of aminopyridine derivatives, reaction of **6** (1.000 g, 3.39 mmol) and trifluoromethanesulfonic acid (5.080 g, 33.88 mmol) in dichloromethane (27 mL) after 2.5 h yielded compound **8** (679 mg, 98%) as a yellow solid. IR (KBr) ν 3390, 3333, 3140, 2973, 2226, 1719, 1672, 1599, 1549, 1400, 1369, 1338, 1291, 1265, 1172, 1069, 943, 779, 556 cm^{-1}; ^1H NMR ($CDCl_3$, 200 MHz) δ 8.32 (s, 1 H, H4), 5.50 (br, 2 H, NH_2), 4.33 (q, J = 7.0 Hz, 2 H, $CO_2CH_2CH_3$), 2.74 [s, 3 H, CH_3(C2)], 1.38 (t, 3 H, J = 7.0 Hz, $CO_2CH_2CH_3$); ^{13}C NMR ($CDCl_3$, 75.4 MHz) δ 166.5, 165.0 (CO, C6), 159.7 (C2), 145.1 (C4), 116.3, 116.2 (C3, CN), 88.9 (C5), 61.5 ($CO_2CH_2CH_3$), 25.9 [CH_3(C2)], 14.7 ($CO_2CH_2CH_3$). MS (API-ES+) m/z: $[M + 1]^+$ 206.0. Anal. ($C_{10}H_{11}N_3O_2$) C, H, N.

General Method of Friedländer Reaction for the Synthesis of [1,8]Naphthyridine Derivatives. Aluminum chloride (1.2−2.2 equiv) was suspended in dry 1,2-dichloroethane (10 mL/mmol) under argon. The corresponding alkyl 6-amino-5-cyano-2-methyl-3-pyridinecarboxylate (1 equiv) and the cycloalkanone (1.2−2.2 equiv) were added. The reaction mixture was heated under reflux (27−49 h). After the reaction was complete (TLC analysis), the mixture was allowed to cool to room temperature and a mixture of THF/H_2O (2:1) was added. An aqueous solution of 10% NaOH was added dropwise to the mixture until the aqueous solution was basic (pH 9). After being stirred for 30 min, the mixture was extracted three times with dichloromethane. The organic layer was washed with brine, dried over anhydrous sodium sulfate, filtered, and the solvent was evaporated. The resultant solid was purified by silica gel flash chromatography using methanol/dichloromethane mixtures as eluent to provide pure compounds.

Methyl Ester of 5-Amino-2-methyl-7,8-dihydro-6*H*-cyclopenta-[*b*][1,8]naphthyridine-3-carboxylic Acid (9). This compound was obtained following the general method for the Friedländer reaction. To a stirred suspension of $AlCl_3$ (93 mg, 0.70 mmol) in dry 1,2-dichloroethane (5 mL) were added methyl 6-amino-5-cyano-2-methyl-3-pyridinecarboxylate **7** (95 mg, 0.50 mmol) and cyclopentanone (59 mg, 0.70 mmol). Upon the TLC analysis, 33 mg of $AlCl_3$ (0.25 mmol) and 21 mg of cyclopentanone (0.25 mmol) were added after 28 h of reflux. The reaction was complete at 49 h of total time, yielding compound **9** (63 mg, 60%) as a yellow solid: mp 255−258 °C; IR (KBr) ν 3317, 3188, 2951, 2844, 1724, 1645, 1601, 1549, 1431, 1358, 1259, 1114, 802, 777 cm^{-1}; ^1H NMR (DMSO-d_6, 200 MHz) δ 9.14 (s, 1 H, H4), 7.03 (br, 2 H, NH_2), 3.89 (s, 3 H, CH_3O), 3.37 (m, 2 H, H8), 2.91 (m, 2 H, H6), 2.79 [s, 3 H, CH_3C(2)], 2.10 (m, 2 H, H7); ^{13}C NMR (DMSO-d_6, 50.2 MHz) δ 171.8 (CO), 166.5 (C8a), 158.9 (C2), 157.0 (C9a), 148.1 (C4), 135.8 (C5), 119.5 (C3), 114.1 (C5a), 109.0 (C4a), 52.1 (CH_3O), 35.1 (C8), 27.5 [CH_3C(2)], 25.3 (C6), 21.8 (C7). MS (API-ES+) m/z: 258.1 [$(M + 1)^+$, 100], 245.1, 205.1, 157.1. Anal. ($C_{14}H_{15}N_3O_2$) C, H, N.

Methyl 5-Amino-2-methyl-6,7,8,9-tetrahydrobenzo[*b*][1,8]naphthyridine-3-carboxylate (10). This compound was obtained following the general method for the Friedländer reaction. To a stirred suspension of $AlCl_3$ (83 mg, 0.62 mmol) in dry 1,2-dichloroethane (5 mL) were added methyl 6-amino-5-cyano-2-methyl-3-pyridinecarboxylate **7** (85 mg, 0.44 mmol) and cyclohexanone (61 mg, 0.62 mmol). Upon the TLC analysis, an amount of 30 mg of $AlCl_3$ (0.22 mmol) was added after 6 h of reflux. Then 30 mg of $AlCl_3$ (0.22 mmol) and 22 mg of cyclohexanone (0.22 mmol) were added after 21 h of reflux. The reaction was complete at 30 h of total time, yielding compound **10** (85 mg, 70%) as a yellow solid: mp >300 °C (dark at 185 °C); IR (KBr) ν 3338, 3229, 2941, 2862, 1716, 1620, 1601, 1568, 1543, 1437, 1361, 1284, 1246, 1116, 1070, 802, 779 cm^{-1}; ^1H NMR ($CDCl_3$, 200 MHz) δ 8.82 (s, 1H, H4), 5.19 (bs, 2H, NH_2), 3.94 (s, 3H, CH_3O), 3.07 (m, 2H, H9), 2.95 [s, 3H, CH_3C(2)], 2.59 (m, 2H, H6), 1.93 (m, 4H, H7, H8); ^{13}C NMR (DMSO-d_6, 75.4 MHz) δ 166.4 (CO), 161.9 (C9a), 159.6 (C2), 154.1 (C10a), 150.9 (C5), 136.0 (C4), 119.7 (C3), 109.9 (C5a), 108.3 (C4a), 52.1 (CH_3O), 33.4 (C9), 25.2 [CH_3C(2)], 23.3 (C6), 22.1, 22.0 (C7, C8). MS (API-ES+) m/z: 272 [$(M + 1)^+$, 100], 248 (12), 205 (13). Anal. ($C_{15}H_{17}N_3O_2$) C, H, N.

Methyl 5-Amino-2-methyl-7,8,9,10-tetrahydro-6*H*-cyclohepta-[*b*][1,8]naphthyridine-3-carboxylate (11). This compound was obtained following the general method for the Friedländer reaction. To a stirred suspension of $AlCl_3$ (93 mg, 0.70 mmol) in dry 1,2-dichloroethane (5 mL) were added methyl 6-amino-5-cyano-2-methyl-3-pyridinecarboxylate **7** (95 mg, 0.50 mmol) and cycloheptanone (78 mg, 0.70 mmol). Upon the TLC analysis, 33 mg of $AlCl_3$ (0.25 mmol) and 28 mg of cycloheptanone (0.25 mmol) were added after 19h of reflux. The reaction was complete at 27 h of total time, yielding compound **11** (95 mg, 67%) as a yellow solid: mp 227−233 °C; IR (KBr) ν 3330, 3199, 2918, 2850, 1720, 1651, 1601, 1579, 1543, 1429, 1361, 1346, 1257, 1105, 1082, 810, 779 cm^{-1}; ^1H NMR ($CDCl_3$, 200 MHz) δ 8.77 (s, 1H, H4), 5.03 (bs, 2H, NH_2), 3.96 (s, 3H, CH_3O), 3.19 (m, 2H, H10), 2.96 [s, 3H, CH_3C(2)], 2.75 (m, 2H, H6), 1.98−1.46 (m, 6H, H7, H8, H9); ^{13}C NMR (DMSO-d_6, 75.4 MHz)

δ 169.1 (CO), 166.4 (C10a), 159.0 (C2), 154.5 (C11a), 149.2 (C5), 136.0 (C4), 120.1 (C3), 114.9 (C5a), 109.2 (C4a), 52.0 (OCH_3), 39.2 (C10), 31.4 (C9), 27.3 (C8), 26.2 (C6), 25.0, 24.9 [$CH_3C(2)$, C7]. MS (API-ES+) *m/z*: 286 [$(M + 1)^+$, 100], 248 (12), 205 (15). HRMS calcd for $C_{16}H_{20}N_3O_2$ 286.1550 ($M + H^+$). Found 286.1544 ($M + H^+$).

Methyl 5-Amino-2-methyl-6,7,8,9,10,11-hexahydrocycloocta-[*b*][1,8]naphthyridine-3-carboxylate (12). This compound was obtained following the general method for the Friedländer reaction. To a stirred suspension of $AlCl_3$ (146 mg, 1.10 mmol) in dry 1,2-dichloroethane (8 mL) were added methyl 6-amino-5-cyano-2-methyl-3-pyridinecarboxylate **7** (150 mg, 0.78 mmol) and cyclooctanone (139 mg, 1.10 mmol). Upon the TLC analysis, 52 mg of $AlCl_3$ (0.39 mmol) and 50 mg of cyclooctanone (0.39 mmol) were added after 20 h of reflux. The reaction was complete at 28 h of total time, yielding compound **12** (134 mg, 57%) as a white solid: mp 259−262 °C; IR (KBr) ν 3349, 2923, 2851, 1725, 1713, 1620, 1600, 1571, 1541, 1432, 1361, 1351, 1291, 1260, 1249, 1109, 1093 cm^{-1}; ^1H NMR ($CDCl_3$, 200 MHz) δ 8.80 (s, 1H, H4), 5.10 (bs, 2H, NH_2), 3.97 (s, 3H, CH_3O), 3.15 (m, 2H, H11), 2.98 [s, 3H, $CH_3C(2)$], 2.88 (m, 2H, H6), 1.90 (m, 2H, H10), 1.73 (m, 2H, H7), 1.43 (m, 4H, H8, H9); ^{13}C NMR ($CDCl_3$, 75.4 MHz) δ 167.6 (CO), 166.5 (C11a), 161.9 (C2), 148.2 (C12a), 146.2 (C5), 134.9 (C4), 121.4 (C3), 114.2 (C5a), 109.0 (C4a), 52.4 (OCH_3), 36.2 (C11), 30.8 (C10), 27.8 (C7), 26.3, 26.2 (C8, C9), 25.9 [$CH_3C(2)$], 24.7 (C6). MS (API-ES+) *m/z*: 300.3 $[(M + 1)^+$, 100], 322.3 $[(M + Na)^+$, 13]. Anal. ($C_{17}H_{21}N_3O_2$) C, H, N.

Ethyl 5-Amino-2-methyl-7,8-dihydro-6*H*-cyclopenta[*b*][1,8]-naphthyridine-3-carboxylate (13). This compound was obtained following the general method for the Friedländer reaction. To a stirred suspension of $AlCl_3$ (91 mg, 0.68 mmol) in dry 1,2-dichloroethane **8** (5 mL) were added ethyl 6-amino-5-cyano-2-methyl-3-pyridinecarboxylate (100 mg, 0.49 mmol) and cyclopentanone (57 mg, 0.68 mmol). Upon the TLC analysis, 32 mg of $AlCl_3$ (0.24 mmol) and 20 mg of cyclopentanone (0.24 mmol) were added after 14 and 25 h of reflux. The reaction was complete at 40 h of total time, yielding compound **13** (91 mg, 69%) as a yellow solid: mp 237−240 °C; IR (KBr) ν 3329, 3176, 2964, 1716, 1657, 1604, 1550, 1433, 1400, 1358, 1252, 1217, 1117, 1086, 1051, 806, 779 cm^{-1}; ^1H NMR ($CDCl_3$, 200 MHz) δ 8.74 (s, 1H, H4), 4.80 (bs, 2H, NH_2), 4.44 (q, J = 7.2 Hz, 2H, $CO_2CH_2CH_3$), 3.16 (t, $J_{7,8}$ = 7.6 Hz, 2H, H8), 2.98 [s, 3H, $CH_3C(2)$], 2.88 (t, $J_{6,7}$ = 7.6 Hz, 2H, H6), 2.23 (quintet, 2H, $J_{6,7,8}$ = 7.6 Hz, H7), 1.45 (t, J = 7.2 Hz, 3H, $CO_2CH_2CH_3$); ^{13}C NMR (DMSO-d_6, 50.2 MHz) δ 171.6 (CO), 166.1 (C8a), 158.7 (C2), 156.9 (C9a), 148.0 (C4), 135.6 (C5), 120.0 (C3), 114.0 (C5a), 109.0 (C4a), 60.8 (OCH_2CH_3), 35.0 (C8), 27.5 (C6), 25.2 [$CH_3C(2)$], 21.8 (C7), 14.1 (OCH_2CH_3). MS (API-ES+) *m/z*: 272.2 $[(M + 1)^+$, 100], 258.1 (8), 245.1 (7). Anal. ($C_{15}H_{17}N_3O_2$) C, H, N.

Ethyl 5-Amino-2-methyl-6,7,8,9-tetrahydrobenzo[*b*][1,8]naphthyridine-3-carboxylate (14). This compound was obtained following the general method for the Friedländer reaction. To a stirred suspension of $AlCl_3$ (112 mg, 0.84 mmol) in dry 1,2-dichloroethane (6 mL) were added ethyl 6-amino-5-cyano-2-methyl-3-pyridinecarboxylate **8** (123 mg, 0.60 mmol) and cyclohexanone (82 mg, 0.84 mmol). Upon the TLC analysis, 40 mg of $AlCl_3$ (0.30 mmol) and 30 mg of cyclohexanone (0.30 mmol) were added after 22 h of reflux. The reaction was complete at 31 h, yielding compound **14** (159 mg, 93%) as a yellow solid: mp 212−215; IR (KBr) ν 3374, 3324, 3182, 2934, 1717, 1664, 1602, 1577, 1546, 1434, 1363, 1350, 1252, 1222, 1120, 1072, cm^{-1}; ^1H NMR ($CDCl_3$, 300 MHz) δ 8.82 (s, 1H, H4), 5.33 (bs, 2H, NH_2), 4.39 (q, J = 7.5 Hz, 2H, $CO_2CH_2CH_3$), 3.05 (m, 2H, H9), 2.91 [s, 3H, $CH_3C(2)$], 2.58 (m, 2H, H6), 1.92 (m, 4H, H7, H8), 1.41 (t, J = 7.5 Hz, 3H, $CO_2CH_2CH_3$); ^{13}C NMR ($CDCl_3$, 75.4 MHz) δ 166.7 (CO), 163.9 (C9a), 162.0 (C2), 154.6 (C10a), 149.5 (C5), 135.0 (C4), 121.8 (C3), 111.5 (C5a), 109.0 (C4a), 61.8 (OCH_2CH_3), 34.2 (C9), 26.4 [$CH_3C(2)$], 23.9 (C6), 22.8 (C7, C8), 14.7 (CH_3CH_2O). MS (API-ES+) *m/z*: 286.2 $[(M + 1)^+$, 100], 593.5 $[(2 \times M + Na)^+$, 5], 308.3 $[(M + Na)^+$, 4], 272.2 (10), 258.2 (12). Anal. ($C_{16}H_{19}N_3O_2$) C, H, N.

Ethyl 5-Amino-2-methyl-7,8,9,10-tetrahydro-6*H*-cyclohepta-[*b*][1,8]naphthyridine-3-carboxylate (15). This compound was obtained following the general method for the Friedländer reaction. To a stirred suspension of $AlCl_3$ (100 mg, 0.75 mmol) in dry 1,2-dichloroethane (6 mL) were added ethyl 6-amino-5-cyano-2-methyl-3-pyridinecarboxylate **8** (110 mg, 0.54 mmol) and cycloheptanone (84 mg, 0.75 mmol). Upon the TLC analysis, 36 mg of $AlCl_3$ (0.27 mmol) and 30 mg of cycloheptanone (0.27 mmol) were added after 10 and 24 h of reflux. The reaction was complete at 33 h of total time, yielding compound **15** (130 mg, 80%) as a yellow solid: mp 252−255 °C; IR (KBr) ν 3381, 3327, 3153, 2923, 2850, 1714, 1670, 1603, 1576, 1543, 1344, 1288, 1254, 1223, 1111, 1082, 1049, 812, 781 cm^{-1}; ^1H NMR ($CDCl_3$, 200 MHz) δ 8.75 (s, 1H, H4), 5.03 (bs, 2H, NH_2), 4.44 (q, J = 7.0 Hz, 2H, $CO_2CH_2CH_3$), 3.19 (m, 2H, H10), 2.96 [s, 3H, $CH_3C(2)$], 2.75 (m, 2H, H6), 2.00−1.60 (m, 6H, H7, H8, H9), 1.44 (t, J = 7.0 Hz, 3H, $CO_2CH_2CH_3$); ^{13}C NMR (DMSO-d_6, 75.4 MHz) δ 169.1 (CO), 166.1 (C10a), 158.8 (C2), 154.6 (C11a), 149.1 (C5), 135.9 (C4), 120.5 (C3), 114.9 (C5a), 109.3 (C4a), 60.8 (OCH_2CH_3), 39.2 (C10), 31.5 (C9), 27.3 (C8), 26.2 (C6), 25.1, 25.0 [$CH_3C(2)$, C7], 14.1 (OCH_2CH_3). MS (API-ES+) *m/z*: 300.2 $[(M + 1)^+$, 100], 205.1 (17), 157.1 (13). Anal. ($C_{17}H_{21}N_3O_2$) C, H, N.

Ethyl 5-Amino-2-methyl-6,7,8,9,10,11-hexahydrocycloocta-[*b*][1,8]naphthyridine-3-carboxylate (16). This compound was obtained following the general method for the Friedländer reaction. To a stirred suspension of $AlCl_3$ (73 mg, 0.55 mmol) in dry 1,2-dichloroethane (4 mL) were added ethyl 6-amino-5-cyano-2-methyl-3-pyridinecarboxylate **8** (80 mg, 0.39 mmol) and cyclooctanone (69 mg, 0.55 mmol). Upon the TLC analysis, 26 mg of $AlCl_3$ (0.19 mmol) and 25 mg of cyclooctanone (0.19 mmol) were added after 15 and 21 h of reflux. The reaction was complete at 39 h of total time, yielding compound **16** (110 mg, 90%) as a white solid: mp 241−243 °C; IR (KBr) ν 3345, 2920, 2846, 1716, 1618, 1599, 1570, 1541, 1431, 1356, 1350, 1290, 1259, 1242, 1167, 1107, 1090, 818, 779 cm^{-1}; ^1H NMR ($CDCl_3$, 200 MHz) δ 8.75 (s, 1H, H4), 5.02 (bs, 2H, NH_2), 4.43 (q, J = 7.0 Hz, 2H, $CO_2CH_2CH_3$), 3.14 (m, 2H, H11), 2.97 [s, 3H, $CH_3C(2)$], 2.87 (m, 2H, H6), 1.88 (m, 2H, H10), 1.72 (m, 2H, H7), 1.43 (t, J = 7.0 Hz, 3H, $CO_2CH_2CH_3$), 1.38 (m, 4H, H8, H9); ^{13}C NMR ($CDCl_3$, 75.4 MHz) δ 166.6 (C11a), 166.1 (CO), 159.3 (C2), 154.6 (C12a), 149.9 (C5), 136.0 (C4), 120.5 (C3), 112.5 (C5a), 108.8 (C4a), 60.8 (OCH_2CH_3), 35.7 (C11), 30.7 (C10), 27.8 (C7), 26.0, 25.8 (C8, C9), 25.1 [$CH_3C(2)$], 23.7 (C6), 14.1 (OCH_2CH_3). MS (API-ES+) *m/z*: 314.2 $[(M + 1)^+$, 100], 205.1 (12). Anal. ($C_{18}H_{23}N_3O_2$) C, H, N.

Molecular Modeling. Molecular modeling studies were carried out with QUANTA/CHARMm sofware running on a Silicon Graphics workstation. The OA structure was retrieved from Protein Data Bank and used as template. Tautomers **14a**, **14b**, **14c**, and **14d** were assembled within QUANTA using standard bond lengths and bond angles. With the CHARMm force field[69] and partial atomic charges, the molecular geometries of OA and tautomers **14a**, **14b**, **14c**, and **14d** were each separately energy-minimized using the adopted-based Newton−Raphson algorithm. Structures were considered fully optimized when the energy changes between iterations were less than 0.01 kcal/mol.[70] Tautomers **14a**, **14b**, **14c**, and **14d** were manually aligned on OA, and the superimposition was based on a similar substructure embedded in OA. Then a rigid body fit of tautomers to targeted atoms on OA was done with Quanta. The set of atoms used for the superpositioning is described in Results and Discussion.

The blind docking experiment was carried out on the complex 2IE4 obtained from the Protein Data Bank (PDB). For docking study, initial protein was prepared by removing all water compounds, heteroatoms, and the ligand (okadaic acid) and CHARMm force field was applied using the receptor−ligand

interactions tool in Discovery Studio, version 2.1, software package. The docking of **14d** into PP2Awas performed with the program AUTODOCK VINA.[71] AUTODOCKTOOLS (ADT) (version 1.5.4) was used to add hydrogens and partial charges for protein and ligand using Gasteiger charges. Flexible torsions in the ligand were assigned with the AUTOTORS module, and the acyclic dihedral angles were allowed to rotate freely.

Because VINA uses rectangular boxes for the binding site, the box center was defined and the docking box was displayed using ADT. The docking procedure was applied to whole protein target, without imposing the binding site ("blind docking"). The grid field was a 120 Å cube with grid points separated 1 Å, at the middle of the protein ($x = 60936$; $y = -25558$; $z = -17702$). Default parameters were used except num_modes, which was set to 30. The lowest docking-energy conformations were included in the largest cluster found (which contains 40% of total conformations). Otherwise, the lowest docking-energy conformation was considered as the most stable orientation. Finally, the docking results generated were directly loaded into Discovery Studio, version 2.1.

Biology. Data Analysis. Data are represented as the mean ± standard error of the mean. Comparisons between experimental and control groups were performed by one-way ANOVA followed by Newman−Keuls post hoc test. Differences were considered to be statistically significant when $p < 0.05$. All statistical procedures were carried out using GraphPad Prism software version 5.0 for an IBM compatible computer.

Culture of SH-SY5Y Cells. SH-SY5Y cells were maintained in a 1:1 mixture of F-12 nutrient mixture (Ham12) (Sigma-Aldrich, Madrid, Spain) and Eagle's minimum essential medium (EMEM) supplemented with 15 nonessential amino acids, 1 mM sodium pyruvate, 10% heat-inactivated fetal bovine serum (FBS), 100 units/mL penicillin, and 100 μg/mL streptomycin (reagents from Invitrogen, Madrid, Spain). Cultures were seeded into flasks containing supplemented medium and maintained at 37 °C in a humidified atmosphere of 5% CO_2 and 95% air. For assays, SH-SY5Y cells were subcultured in 48-well plates at a seeding density of 1×10^5 cells per well. Cells were treated with the drugs before confluence in EMEM with 1% FBS. All the cells used in this study were used at a low passage number (< 13).

Incubation of drugs. Concentrated solutions of drugs were prepared in DMSO. For the DMSO group (control), 0.1% DMSO was incubated, having the same DMSO concentration of the tested drugs group. Compounds at 1 μM were administered 24 h before adding the cytotoxic stimuli (rotenone/oligomycin A, okadaic acid, or Aβ). Then cells were co-incubated for another 24 h with the drug in the presence of stimuli. All toxic stimuli were incubated in serum-free EMEM.

Inhibition Experiments of AChE and BuChE. To assess the inhibitory activity of the compounds toward AChE or BuChE, we followed the spectrophotometric method of Ellman,[41] using purified AChE from *Electrophorus electricus* (type V-S), human erythrocytes (buffered aqueous solution) or BuChE from equine serum (lyophilized powder) (Sigma-Aldrich, Madrid, Spain). The reaction took place in a final volume of 3 mL of a phosphate-buffered solution (0.1 M) at pH 8, containing 0.035 U of AChE or 0.05 U of BuChE and 0.35 mM of 5,5′-dithiobis-2-nitrobenzoic acid (DTNB, Sigma-Aldrich, Madrid, Spain). Inhibition curves were made by preincubating this mixture with at least nine concentrations of each compound for 10 min. A sample with no compound was always present to determine the 100% of enzyme activity. After this preincubation period, acetylthiocholine iodide (0.35 mM) or butyrylthiocholine iodide (0.5 mM) (Sigma-Aldrich, Madrid, Spain) was added, allowing 15 min more of incubation, where the DTNB produces the yellow anion 5-thio-2-nitrobenzoic acid along with the enzymatic degradation of acetylthiocholine iodide or butyrylthiocholine iodide. Changes in absorbance were detected at 405 nm in a spectrophotometric plate reader (FluoStar OPTIMA, BMG Labtech). Compounds inhibiting AChE or BuChE activity would reduce the color generation; thus, IC_{50} values were calculated as the concentration of compound that produces 50% AChE activity inhibition. Data are expressed as the mean ± SEM of at least three different experiments in quadruplicate.

Kinetic Analysis of the AChE Inhibition. To obtain estimates of the competitive inhibition constant K_i, reciprocal plots of $1/V$ versus 1/[S] were constructed at different concentrations of the substrate acetylthiocholine (0.1−1 mM) by using Ellman's method.[41] Experiments were performed in a transparent 48-well plate containing in each well 350 μL of the DTNB solution and 1 μL of DMSO (control) or inhibitor solution to give desired final concentration. Reaction was initiated by adding 45 μL of AChE (0.18 U/mL) at 30 °C. Progress curves were monitored at 412 nm over 2 min in a Fluostar Optima (BMG-Technologies, Germany) fluorescence plate reader. Progress curves were characterized by a linear steady-state turnover of the substrate, and values of a linear regression were fitted according to Lineweaver−Burk replots using Origin software. The plots were assessed by a weighted least-squares analysis. Determination of the Michaelis constant for the substrate ATCh was done at seven different concentrations (0.1−1 mM) to give $K_M = 0.64 \pm 0.09$ mM and $V_{max} = 1.7 \pm 0.2$ min^{-1}. Slopes of the reciprocal plots were then plotted against the concentration of **14** (range 0−0.5 μM) as described,[72] to evaluate K_i data. Data analysis was performed with Origin Pro 7.5 software (Origin Lab Corp.).

Measurement of Cytosolic Ca^{2+} Concentrations, $[Ca^{2+}]_c$. SH-SY5Y neuroblastoma cells were grown at confluence in 96-well black dishes. Cells were loaded with 4 μM Fluo-4/AM for 1 h at 37 °C in EMEM. Then cells were washed twice with Krebs Hepes solution and kept at room temperature for 15 min before the beginning of the experiment. Compounds were incubated 10 min before K^+ (70 mM) was applied to evoke the increment of $[Ca^{2+}]_c$. At the end of the experiment, Triton X-100 (5%) and 1 mM $MnCl_2$ were applied to record maximal and basal fluorescence, respectively. Fluorescence was measured in a fluorescence microplate reader (FLUOstar Optima, BMG, Germany). Wavelengths of excitation and emission were 485 and 520 nm, respectively.

Measurement of LDH Activity. LDH activity was spectrophotometrically measured using a cytotoxicity cell death kit (Roche-Boehringer, Mannheim, Germany) according to the manufacturer's indications. Total LDH activity was defined as the sum of intracellular and extracellular LDH activity. Released LDH was defined as the percentage of extracellular compared to total LDH activity. At the end of the toxic stimulus exposition (24 h), samples were collected to estimate extracellular LDH as indication of cell death.[53,65] Intracellular LDH activity was measured in the cells after incubation with 10% Triton X-100. LDH activity was measured at 490 and 620 nm, using a microplate reader (Labsystems iEMS reader MF; Labsystems, Helsinki, Finland). Total LDH (intracellular plus extracellular) was normalized to 100%. Then the amount of LDH released to the extracellular medium was expressed as a percentage of this total. Data were normalized by subtracting basal LDH (cells not subjected to any treatment) from the different treatment groups in each individual experiment, and the result for the Rot/Olig group was normalized to 100% (percentage cell death).

Quantification of Viability by MTT in SH-SY5Y Cells. Cell viability, virtually the mitochondrial activity of living cells, was measured by quantitative colorimetric assay with MTT (3-[4,5-dimethylthiazol-2-yl]-2,5-diphenyltetrazolium bromide, Sigma-Aldrich, Madrid, Spain), as described previously.[57] SH-SY5Y cells were seeded into 48-well culture plates and allowed to attach. MTT was added to all wells (5 mg/mL) and allowed to incubate in the dark at 37 °C for 2 h followed by cell lysis and spectrophotometric measurement at 540 nm. The tetrazolium ring of MTT can be cleaved by active reductases in order to produce a precipitated formazan derivative. The formazan produced was dissolved by adding 200 μL of DMSO, resulting

in a colored compound whose optical density was measured in an ELISA reader at 540 nm. All MTT assays were performed in triplicate.

In Vitro Malachite Green Phosphatase Assay. Cortex were homogenized and lysed in 20 mM imidazole−HCl, 2 mM EDTA, 2 mM EGTA, pH 7.0, with 10 μg/mL leupeptin, 1 mM PMSF, and protease inhibitor cocktail. An amount of 500 μg of whole lysates was used to immunoprecipitate PP2A with an antibody against the subunit C of PP2A and protein A/agarose following the protocol of PP2A immunoprecipitation phosphatase assay kit (Millipore). Subsequently, the beads were washed three times with the above lysis buffer and twice with the phosphatase assay buffer (50 mM Tris-HCl, pH 7.0, 0.1 mM $CaCl_2$). The phosphatase activity of immunoprecipitated PP2A was assayed using Lys-Arg-pThr-Ile-Arg-Arg as the enzymatic substrate provided, following the manufacturer's instructions. Absorbance was measured at 620 nm using a microplate reader (Labsystems iEMS reader MF). Assays were performed in triplicate.

Viability in Hippocampal Slices Preparations. We followed the protocol described by Egea and co-workers[73] with slight modifications. Rats were quickly decapitated under sodium pentobarbital anesthesia (60 mg/kg, ip). Forebrains were rapidly removed from the skull and placed into ice-cold Krebs bicarbonate dissection buffer (pH 7.4) containing the following: NaCl 120 mM, KCl 2 mM, $CaCl_2$ 0.5 mM, $NaHCO_3$ 26 mM, $MgSO_4$ 10 mM, KH_2PO_4 1.18 mM, glucose 11 mM, and sucrose 200 mM. The hippocampi were quickly dissected, and slices (350 μm thick) were rapidly prepared using a McIlwain tissue chopper, separated in Krebs buffer at 4 °C, and allowed to recover for 45 min in Krebs bicarbonate buffer at 37 °C. For OGD experiments, after an initial preincubation period of 30 min, hippocampal slices corresponding to the control group were incubated for 15 min in a Krebs solution with the following composition: NaCl 120 mM, KCl 2 mM, $CaCl_2$ 2 mM, $NaHCO_3$ 26 mM, $MgSO_4$ 1.19 mM, KH_2PO_4 1.18 mM, and glucose 11 mM. This solution was equilibrated with 95% O_2 and 5% CO_2. OGD was induced by incubating the slices in a glucose-free Krebs solution, equilibrated with a 95% N_2 and 5% CO_2 gas mixture. Glucose was replaced by 2-deoxyglucose. After this OGD period, the slices were returned to an oxygenated normal Krebs solution containing glucose (reoxygenation period). Experiments were performed at 37 °C. A control and OGD group was included in all experiments. The OGD−reoxygenation protocol was 15 min OGD followed by 120 min reoxygenation. Hippocampal slice viability was determined through the ability of the cells to reduce MTT.[74] Hippocampal slices were collected immediately after the reoxygenation period and were incubated with MTT (0.5 mg/mL) in Krebs bicarbonate solution for 30 min at 37 °C. Formazan production was measured as described above.

Acknowledgment. C.d.l.R. thanks Ministerio de Ciencia e Innovación for a "Juan de la Cierva" contract. A.S. thanks CSIC for an I3P postdoctoral contract. The present work was supported by the Comunidad Autónoma de Madrid CAM (Grant S/SAL-0275-2006) and Instituto de Salud Carlos III (MICINN, Spain) [RETIC "RENEVAS" (Grants RD06/0026/0009, RD06/0026/1002). M.G.L. (Grant SAF2009-12150) and J.M.-C. (Grants SAF2006-08764-C02-01, SAF-2009-07271) thank Spanish Ministry of Science and Innovation for financial support. This work was supported in part by grants to A.G.G.: (1) Fundación C.I.E.N., Instituto de Salud Carlos III, MICINN; (2) Grant NDE 07/09, Agencia Laín Entralgo, Comunidad de Madrid; (3) Grant SAF2006-03589, MICINN, Spain.

Supporting Information Available: Elemental analysis results for compounds **9**−**16**, results and experimental details of the propidium displacement assay, full data of Ca^{2+} channel blocking activity of **9**−**16**, tables of results for all neuroprotection experiments, protocol of animal usage, and references. This material is available free of charge via the Internet at http://pubs.acs.org.

References

(1) Goedert, M.; Spillantini, M. G. A century of Alzheimer's disease. *Science* **2006**, *314*, 777–781.
(2) Castro, A.; Martinez, A. Targeting beta-amyloid pathogenesis through acetylcholinesterase inhibitors. *Curr. Pharm. Des.* **2006**, *12*, 4377–4387.
(3) Gong, C. X.; Iqbal, K. Hyperphosphorylation of microtubule-associated protein tau: a promising therapeutic target for Alzheimer disease. *Curr. Med. Chem.* **2008**, *15*, 2321–2328.
(4) Pratico, D. Evidence of oxidative stress in Alzheimer's disease brain and antioxidant therapy: lights and shadows. *Ann. N.Y. Acad. Sci.* **2008**, *1147*, 70–78.
(5) Cummings, J. L. Treatment of Alzheimer's disease: current and future therapeutic approaches. *Rev. Neurol. Dis.* **2004**, *1*, 60–69.
(6) Rafii, M. S.; Aisen, P. S. Recent developments in Alzheimer's disease therapeutics. *BMC Med.* **2009**, *7*, 7.
(7) van Marum, R. J. Current and future therapy in Alzheimer's disease. *Fundam. Clin. Pharmacol.* **2008**, *22*, 265–274.
(8) Fillit, H. M.; Doody, R. S.; Binaso, K.; Crooks, G. M.; Ferris, S. H.; Farlow, M. R.; Leifer, B.; Mills, C.; Minkoff, N.; Orland, B.; Reichman, W. E.; Salloway, S. Recommendations for best practices in the treatment of Alzheimer's disease in managed care. *Am. J. Geriatr. Pharmacother.* **2006**, *4* (Suppl. A), S9−S24; quiz S25−S28.
(9) Racchi, M.; Mazzucchelli, M.; Porrello, E.; Lanni, C.; Govoni, S. Acetylcholinesterase inhibitors: novel activities of old molecules. *Pharmacol. Res.* **2004**, *50*, 441–451.
(10) Talesa, V. N. Acetylcholinesterase in Alzheimer's disease. *Mech. Ageing Dev.* **2001**, *122*, 1961–1969.
(11) O'Neill, M. F. Difficult times for Alzheimer's treatments. *Drug Discovery Today* **2005**, *10*, 1333–1335.
(12) Bullock, R.; Touchon, J.; Bergman, H.; Gambina, G.; He, Y.; Rapatz, G.; Nagel, J.; Lane, R. Rivastigmine and donepezil treatment in moderate to moderately-severe Alzheimer's disease over a 2-year period. *Curr. Med. Res. Opin.* **2005**, *21*, 1317–1327.
(13) Li, W.; Mak, M.; Jiang, H.; Wang, Q.; Pang, Y.; Chen, K.; Han, Y. Novel anti-Alzheimer's dimer bis(7)-cognitin: cellular and molecular mechanisms of neuroprotection through multiple targets. *Neurotherapeutics* **2009**, *6*, 187–201.
(14) Lorrio, S.; Sobrado, M.; Arias, E.; Roda, J. M.; Garcia, A. G.; Lopez, M. G. Galantamine postischemia provides neuroprotection and memory recovery against transient global cerebral ischemia in gerbils. *J. Pharmacol. Exp. Ther.* **2007**, *322*, 591–599.
(15) Arias, E.; Ales, E.; Gabilan, N. H.; Cano-Abad, M. F.; Villarroya, M.; Garcia, A. G.; Lopez, M. G. Galantamine prevents apoptosis induced by beta-amyloid and thapsigargin: involvement of nicotinic acetylcholine receptors. *Neuropharmacology* **2004**, *46*, 103–114.
(16) Melo, J. B.; Sousa, C.; Garcao, P.; Oliveira, C. R.; Agostinho, P. Galantamine protects against oxidative stress induced by amyloid-beta peptide in cortical neurons. *Eur. J. Neurosci.* **2009**, *29*, 455–464.
(17) Noh, M. Y.; Koh, S. H.; Kim, Y.; Kim, H. Y.; Cho, G. W.; Kim, S. H. Neuroprotective effects of donepezil through inhibition of GSK-3 activity in amyloid-beta-induced neuronal cell death. *J. Neurochem.* **2009**, *108*, 1116–1125.
(18) Inestrosa, N. C.; Alvarez, A.; Perez, C. A.; Moreno, R. D.; Vicente, M.; Linker, C.; Casanueva, O. I.; Soto, C.; Garrido, J. Acetylcholinesterase accelerates assembly of amyloid-beta-peptides into Alzheimer's fibrils: possible role of the peripheral site of the enzyme. *Neuron* **1996**, *16*, 881–891.
(19) Bartolini, M.; Bertucci, C.; Cavrini, V.; Andrisano, V. beta-Amyloid aggregation induced by human acetylcholinesterase: inhibition studies. *Biochem. Pharmacol.* **2003**, *65*, 407–416.
(20) Espinoza-Fonseca, L. M. The benefits of the multi-target approach in drug design and discovery. *Bioorg. Med. Chem.* **2006**, *14*, 896–897.
(21) Cavalli, A.; Bolognesi, M. L.; Minarini, A.; Rosini, M.; Tumiatti, V.; Recanatini, M.; Melchiorre, C. Multi-target-directed ligands to combat neurodegenerative diseases. *J. Med. Chem.* **2008**, *51*, 347–372.
(22) Camps, P.; Formosa, X.; Galdeano, C.; Gomez, T.; Munoz-Torrero, D.; Scarpellini, M.; Viayna, E.; Badia, A.; Clos, M. V.; Camins, A.; Pallas, M.; Bartolini, M.; Mancini, F.; Andrisano, V.; Estelrich, J.; Lizondo, M.; Bidon-Chanal, A.; Luque, F. J. Novel

donepezil-based inhibitors of acetyl- and butyrylcholinesterase and acetylcholinesterase-induced beta-amyloid aggregation. *J. Med. Chem.* **2008**, *51*, 3588–3598.
(23) Piazzi, L.; Cavalli, A.; Colizzi, F.; Belluti, F.; Bartolini, M.; Mancini, F.; Recanatini, M.; Andrisano, V.; Rampa, A. Multi-target-directed coumarin derivatives: hAChE and BACE1 inhibitors as potential anti-Alzheimer compounds. *Bioorg. Med. Chem. Lett.* **2008**, *18*, 423–426.
(24) Camps, P.; Formosa, X.; Galdeano, C.; Munoz-Torrero, D.; Ramirez, L.; Gomez, E.; Isambert, N.; Lavilla, R.; Badia, A.; Clos, M. V.; Bartolini, M.; Mancini, F.; Andrisano, V.; Arce, M. P.; Rodriguez-Franco, M. I.; Huertas, O.; Dafni, T.; Luque, F. J. Pyrano[3,2-*c*]quinoline-6-chlorotacrine hybrids as a novel family of acetylcholinesterase- and beta-amyloid-directed anti-Alzheimer compounds. *J. Med. Chem.* **2009**, *52*, 5365–5379.
(25) Weinstock, M.; Kirschbaum-Slager, N.; Lazarovici, P.; Bejar, C.; Youdim, M. B.; Shoham, S. Neuroprotective effects of novel cholinesterase inhibitors derived from rasagiline as potential anti-Alzheimer drugs. *Ann. N.Y. Acad. Sci.* **2001**, *939*, 148–161.
(26) de los Rios, C.; Marco, J. L.; Carreiras, M. D.; Chinchon, P. M.; Garcia, A. G.; Villarroya, M. Novel tacrine derivatives that block neuronal calcium channels. *Bioorg. Med. Chem.* **2002**, *10*, 2077–2088.
(27) Marco, J. L.; de los Rios, C.; Carreiras, M. C.; Banos, J. E.; Badia, A.; Vivas, N. M. Synthesis and acetylcholinesterase/butyrylcholinesterase inhibition activity of new tacrine-like analogues. *Bioorg. Med. Chem.* **2001**, *9*, 727–732.
(28) Marco-Contelles, J.; Leon, R.; de Los Rios, C.; Guglietta, A.; Terencio, J.; Lopez, M. G.; Garcia, A. G.; Villarroya, M. Novel multipotent tacrine−dihydropyridine hybrids with improved acetylcholinesterase inhibitory and neuroprotective activities as potential drugs for the treatment of Alzheimer's disease. *J. Med. Chem.* **2006**, *49*, 7607–7610.
(29) Marco-Contelles, J.; Leon, R.; de los Rios, C.; Samadi, A.; Bartolini, M.; Andrisano, V.; Huertas, O.; Barril, X.; Luque, F. J.; Rodriguez-Franco, M. I.; Lopez, B.; Lopez, M. G.; Garcia, A. G.; Carreiras Mdo, C.; Villarroya, M. Tacripyrines, the first tacrine−dihydropyridine hybrids, as multitarget-directed ligands for the treatment of Alzheimer's disease. *J. Med. Chem.* **2009**, *52*, 2724–2732.
(30) Summers, W. K.; Majovski, L. V.; Marsh, G. M.; Tachiki, K.; Kling, A. Oral tetrahydroaminoacridine in long-term treatment of senile dementia, Alzheimer type. *N. Engl. J. Med.* **1986**, *315*, 1241–1245.
(31) Mori, Y.; Mikala, G.; Varadi, G.; Kobayashi, T.; Koch, S.; Wakamori, M.; Schwartz, A. Molecular pharmacology of voltage-dependent calcium channels. *Jpn. J. Pharmacol.* **1996**, *72*, 83–109.
(32) Kobayashi, T.; Mori, Y. Ca^{2+} channel antagonists and neuroprotection from cerebral ischemia. *Eur. J. Pharmacol.* **1998**, *363*, 1–15.
(33) Lukic-Panin, V.; Kamiya, T.; Zhang, H.; Hayashi, T.; Tsuchiya, A.; Sehara, Y.; Deguchi, K.; Yamashita, T.; Abe, K. Prevention of neuronal damage by calcium channel blockers with antioxidative effects after transient focal ischemia in rats. *Brain Res.* **2007**, *1176*, 143–150.
(34) Marco, J. L.; de los Rios, C.; Garcia, A. G.; Villarroya, M.; Carreiras, M. C.; Martins, C.; Eleuterio, A.; Morreale, A.; Orozco, M.; Luque, F. J. Synthesis, biological evaluation and molecular modelling of diversely functionalized heterocyclic derivatives as inhibitors of acetylcholinesterase/butyrylcholinesterase and modulators of Ca^{2+} channels and nicotinic receptors. *Bioorg. Med. Chem.* **2004**, *12*, 2199–2218.
(35) Orozco, C.; de Los Rios, C.; Arias, E.; Leon, R.; Garcia, A. G.; Marco, J. L.; Villarroya, M.; Lopez, M. G. ITH4012 (ethyl 5-amino-6,7,8,9-tetrahydro-2-methyl-4-phenylbenzol[1,8]naphthyridine-3-carboxylate), a novel acetylcholinesterase inhibitor with "calcium promotor" and neuroprotective properties. *J. Pharmacol. Exp. Ther.* **2004**, *310*, 987–994.
(36) Abushanab, F. A.; Aly, F. M.; Wakefield, B. J. Synthesis of substituted nicotinamides from enamines derived from *N*,*N*-dimethylformamide dimethyl acetal. *Synthesis* **1995**, 923–925.
(37) Crey-Desbiolles, C.; Kotera, M. Synthesis of 3-deaza-3-nitro-2′-deoxyadenosine. *Bioorg. Med. Chem.* **2006**, *14*, 1935–1941.
(38) Sunthankar, S. V.; Vaidya, S. D. Some reactions of 5-carbethoxy-3-cyano-6-methyl-2-pyridone. *Indian J. Chem., Sect. B: Org. Chem. Incl. Med. Chem.* **1977**, *15*, 187–188.
(39) Minetti, P.; Tinti, M. O.; Carminati, P.; Castorina, M.; Di Cesare, M. A.; Di Serio, S.; Gallo, G.; Ghirardi, O.; Giorgi, F.; Giorgi, L.; Piersanti, G.; Bartoccini, F.; Tarzia, G. 2-*n*-Butyl-9-methyl-8-[1,2,3]triazol-2-yl-9*H*-purin-6-ylamine and analogues as A2A adenosine receptor antagonists. Design, synthesis, and pharmacological characterization. *J. Med. Chem.* **2005**, *48*, 6887–6896.
(40) Cheng, C. C.; Yan, S. J. The Friedlander synthesis of quinolines. *Org. React.* **1982**, *28*, 37–201.
(41) Ellman, G. L.; Courtney, K. D.; Andres, V., Jr.; Feather-Stone, R. M. A new and rapid colorimetric determination of acetylcholinesterase activity. *Biochem. Pharmacol.* **1961**, *7*, 88–95.
(42) Bourne, Y.; Grassi, J.; Bougis, P. E.; Marchot, P. Conformational flexibility of the acetylcholinesterase tetramer suggested by X-ray crystallography. *J. Biol. Chem.* **1999**, *274*, 30370–30376.
(43) Ott, P.; Lustig, A.; Brodbeck, U.; Rosenbusch, J. P. Acetylcholinesterase from human erythrocytes membranes: dimers as functional units. *FEBS Lett.* **1982**, *138*, 187–189.
(44) Liao, J.; Heider, H.; Sun, M. C.; Brodbeck, U. Different glycosylation in acetylcholinesterases from mammalian brain and erythrocytes. *J. Neurochem.* **1992**, *58*, 1230–1238.
(45) Acheson, S. A.; Quinn, D. M. Anatomy of acetylcholinesterase catalysis: reaction dynamics analogy for human erythrocyte and electric eel enzymes. *Biochim. Biophys. Acta* **1990**, *1040*, 199–205.
(46) Atack, J. R.; Yu, Q. S.; Soncrant, T. T.; Brossi, A.; Rapoport, S. I. Comparative inhibitory effects of various physostigmine analogs against acetyl- and butyrylcholinesterases. *J. Pharmacol. Exp. Ther.* **1989**, *249*, 194–202.
(47) Andersen, R. A.; Aaraas, I.; Gaare, G.; Fonnum, F. Inhibition of acetylcholinesterase from different species by organophosphorus compounds, carbamates and methylsulphonyfluoride. *Gen. Pharmacol.* **1977**, *8*, 331–334.
(48) Chan, S. L.; Shirachi, D. Y.; Bhargava, H. N.; Gardner, E.; Trevor, A. J. Purifcation and properties of multiple forms of brain acetylcholinesterase (EC 3.1.1.7). *J. Neurochem.* **1972**, *19*, 2747–2758.
(49) Rampa, A.; Bisi, A.; Belluti, F.; Gobbi, S.; Valenti, P.; Andrisano, V.; Cavrini, V.; Cavalli, A.; Recanatini, M. Acetylcholinesterase inhibitors for potential use in Alzheimer's disease: molecular modeling, synthesis and kinetic evaluation of 11*H*-indeno-[1,2-*b*]-quinolin-10-ylamine derivatives. *Bioorg. Med. Chem.* **2000**, *8*, 497–506.
(50) Rosenberry, T. L.; Mallender, W. D.; Thomas, P. J.; Szegletes, T. A steric blockade model for inhibition of acetylcholinesterase by peripheral site ligands and substrate. *Chem.-Biol. Interact.* **1999**, *119−120*, 85–97.
(51) Berridge, M. J. Calcium hypothesis of Alzheimer's disease. *Pfluegers Arch.* **2010**, *459*, 441−449.
(52) Egea, J.; Rosa, A. O.; Cuadrado, A.; Garcia, A. G.; Lopez, M. G. Nicotinic receptor activation by epibatidine induces heme oxygenase-1 and protects chromaffin cells against oxidative stress. *J. Neurochem.* **2007**, *102*, 1842–1852.
(53) Koh, J. Y.; Choi, D. W. Quantitative determination of glutamate mediated cortical neuronal injury in cell culture by lactate dehydrogenase efflux assay. *J. Neurosci. Methods* **1987**, *20*, 83–90.
(54) Dodd, S.; Dean, O.; Copolov, D. L.; Malhi, G. S.; Berk, M. *N*-Acetylcysteine for antioxidant therapy: pharmacology and clinical utility. *Expert Opin. Biol. Ther.* **2008**, *8*, 1955–1962.
(55) Arendt, T.; Holzer, M.; Bruckner, M. K.; Janke, C.; Gartner, U. The use of okadaic acid in vivo and the induction of molecular changes typical for Alzheimer's disease. *Neuroscience* **1998**, *85*, 1337–1340.
(56) Sun, L.; Liu, S. Y.; Zhou, X. W.; Wang, X. C.; Liu, R.; Wang, Q.; Wang, J. Z. Inhibition of protein phosphatase 2A- and protein phosphatase 1-induced tau hyperphosphorylation and impairment of spatial memory retention in rats. *Neuroscience* **2003**, *118*, 1175–1182.
(57) Denizot, F.; Lang, R. Rapid colorimetric assay for cell growth and survival. Modifications to the tetrazolium dye procedure giving improved sensitivity and reliability. *J. Immunol. Methods* **1986**, *89*, 271–277.
(58) Arias, E.; Gallego-Sandin, S.; Villarroya, M.; Garcia, A. G.; Lopez, M. G. Unequal neuroprotection afforded by the acetylcholinesterase inhibitors galantamine, donepezil, and rivastigmine in SH-SY5Y neuroblastoma cells: role of nicotinic receptors. *J. Pharmacol. Exp. Ther.* **2005**, *315*, 1346–1353.
(59) Sheppeck, J. E., 2nd; Gauss, C. M.; Chamberlin, A. R. Inhibition of the Ser-Thr phosphatases PP1 and PP2A by naturally occurring toxins. *Bioorg. Med. Chem.* **1997**, *5*, 1739–1750.
(60) Harder, K. W.; Owen, P.; Wong, L. K.; Aebersold, R.; Clark-Lewis, I.; Jirik, F. R. Characterization and kinetic analysis of the intracellular domain of human protein tyrosine phosphatase beta (HPTP beta) using synthetic phosphopeptides. *Biochem. J.* **1994**, *298* (Part 2), 395–401.
(61) Begum, N.; Ragolia, L. cAMP counter-regulates insulin-mediated protein phosphatase-2A inactivation in rat skeletal muscle cells. *J. Biol. Chem.* **1996**, *271*, 31166–31171.
(62) Jarrett, J. T.; Berger, E. P.; Lansbury, P. T., Jr. The C-terminus of the beta protein is critical in amyloidogenesis. *Ann. N.Y. Acad. Sci.* **1993**, *695*, 144–148.

(63) Pappolla, M. A.; Sos, M.; Omar, R. A.; Bick, R. J.; Hickson-Bick, D. L.; Reiter, R. J.; Efthimiopoulos, S.; Robakis, N. K. Melatonin prevents death of neuroblastoma cells exposed to the Alzheimer amyloid peptide. *J. Neurosci.* **1997**, *17*, 1683–1690.
(64) Masilamoni, J. G.; Jesudason, E. P.; Dhandayuthapani, S.; Ashok, B. S.; Vignesh, S.; Jebaraj, W. C.; Paul, S. F.; Jayakumar, R. The neuroprotective role of melatonin against amyloid beta peptide injected mice. *Free Radical Res.* **2008**, *42*, 661–673.
(65) Sobrado, M.; Roda, J. M.; Lopez, M. G.; Egea, J.; Garcia, A. G. Galantamine and memantine produce different degrees of neuroprotection in rat hippocampal slices subjected to oxygen−glucose deprivation. *Neurosci. Lett.* **2004**, *365*, 132–136.
(66) Doody, R. S.; Gavrilova, S. I.; Sano, M.; Thomas, R. G.; Aisen, P. S.; Bachurin, S. O.; Seely, L.; Hung, D. Effect of dimebon on cognition, activities of daily living, behaviour, and global function in patients with mild-to-moderate Alzheimer's disease: a randomised, double-blind, placebo-controlled study. *Lancet* **2008**, *372*, 207–215.
(67) Bachurin, S. O.; Shevtsova, E. P.; Kireeva, E. G.; Oxenkrug, G. F.; Sablin, S. O. Mitochondria as a target for neurotoxins and neuroprotective agents. *Ann. N.Y. Acad. Sci.* **2003**, *993*, 334–344; discussion 345−339 .
(68) Lermontova, N. N.; Redkozubov, A. E.; Shevtsova, E. F.; Serkova, T. P.; Kireeva, E. G.; Bachurin, S. O. Dimebon and tacrine inhibit neurotoxic action of beta-amyloid in culture and block L-type Ca(2+) channels. *Bull. Exp. Biol. Med.* **2001**, *132*, 1079–1083.
(69) Brooks, B. R.; Bruccoleri, R. E.; Olafson, B. D.; States, D. J.; Swaminathan, S.; Karplus, M. Charmm, a program for macromolecular energy, minimization, and dynamics calculations. *J. Comput. Chem.* **1983**, *4*, 187–217.
(70) Morreale, A.; Maseras, F.; Iriepa, I.; Galvez, E. Ligand−receptor interaction at the neural nicotinic acetylcholine binding site: a theoretical model. *J. Mol. Graphics Modell.* **2002**, *21*, 111–118.
(71) Trott, O.; Olson, A. J. AutoDock Vina: improving the speed and accuracy of docking with a new scoring function, efficient optimization, and multithreading. *J. Comput. Chem.* **2010**, *31*, 455–461.
(72) Segel, I. H. *Enzyme Kinetics*; John Wiley: Toronto, Canada, 1975.
(73) Egea, J.; Rosa, A. O.; Sobrado, M.; Gandia, L.; Lopez, M. G.; Garcia, A. G. Neuroprotection afforded by nicotine against oxygen and glucose deprivation in hippocampal slices is lost in alpha7 nicotinic receptor knockout mice. *Neuroscience* **2007**, *145*, 866–872.
(74) Mosmann, T. Rapid colorimetric assay for cellular growth and survival: application to proliferation and cytotoxicity assays. *J. Immunol. Methods* **1983**, *65*, 55–63.